

Article

Study of Metallic Housing of the Adder Gearbox to Reduce the Noise and to Improve the Design Solution

Nicoleta Gillich ¹, Nicolae Sîrbu ², Sorin Vlase ^{2,3,*} and Marin Marin ⁴ 

¹ Department for Engineering Science, Faculty of Engineering, Babes-Bolyai University, 400083 Cluj-Napoca, Romania; nicoleta.gillich@ubbcluj.ro

² Department of Mechanics, Transilvania University of Brasov, B-Dul Eroilor 29, 500036 Brasov, Romania; d-mec@unitbv.ro

³ Romanian Academy of Technical Sciences, B-Dul Dacia 26, 030167 Bucharest, Romania

⁴ Department of Mathematics and Informatics, Transilvania University of Brasov, B-Dul Eroilor 29, 500036 Brasov, Romania; m.marin@unitbv.ro

* Correspondence: svlase@unitbv.ro; Tel.: +40-722-643020

Abstract: In the manufacture of commercial trucks, used in oil installations or the army, two identical engines are used on a single chassis, whose power is summed by a gearbox, a compact metal construction, which must meet multiple operating requirements. The paper studies the behavior of such an adding box, currently used in manufacturing, and an improved, welded solution that produces less noise and has a lower weight. The finite element method is used for modeling the gearbox in order to analyze stresses and strains and obtain a modal analysis of the system. The results obtained from the calculation are then verified by experimental measurements. The two versions are analyzed in parallel to highlight the advantages of the second version.

Keywords: adder gearbox; housing; heavy truck; mechanical transmission



Citation: Gillich, N.; Sîrbu, N.; Vlase, S.; Marin, M. Study of Metallic Housing of the Adder Gearbox to Reduce the Noise and to Improve the Design Solution. *Metals* **2021**, *11*, 912. <https://doi.org/10.3390/met11060912>

Academic Editor: Young Jong Kang

Received: 15 May 2021

Accepted: 31 May 2021

Published: 3 June 2021

Publisher's Note: MDPI stays neutral with regard to jurisdictional claims in published maps and institutional affiliations.



Copyright: © 2021 by the authors. Licensee MDPI, Basel, Switzerland. This article is an open access article distributed under the terms and conditions of the Creative Commons Attribution (CC BY) license (<https://creativecommons.org/licenses/by/4.0/>).

1. Introduction

The noise radiated by mechanical transmissions (gearboxes, distribution, connecting elements, drive axles, or final transmissions) is influenced by the judicious choice of parameters and basic design characteristics imposed by considerations of performance, power, weight, and reliability. A proper choice of these alternatives, right from the design phase, can both reduce noise and improve the performance of components and the vehicle as a whole.

The vibrations are transmitted through the internal components (gears, shafts, bearings, pipes, and pumps) to the limit surfaces and then radiated in the form of airborne noise. The box is intended for the drilling chassis equipped with two CATERPILLAR engine groups and an ALLISON automatic gearbox. Special vehicles are vehicles that, in addition to the propulsion system, are composed of a series of units and equipment that ensure the development of multiple activities in different fields.

The adder box is a mechanical construction comprising gears in steps, which has the role of summing the power of the two power groups and distributing it to the drive axles or to a total power take-off. This box ensures both the movement of the vehicle in the field and the drive of a diverse range of units mounted on the chassis. These aggregates perform drilling and extraction of oil and need high driving power and therefore a proper moment. For this reason, the adder box, mounted on the chassis, sums the torque from two engines and develops, through the power take-off, a maximum torque of 40,000 Nm.

Figure 1 shows the special vehicle, fully equipped to be used for oil operations, which consists of the adder box type CSD 4000, built entirely of metal, which is the subject of this work. For the vehicle on which this adder box is mounted, there is a major desideratum: to reduce the weight as much as possible. The research will follow an improved constructive

variant that would allow the weight of the adder box to be reduced without affecting its noise level. The aim of the research is to improve the parameters of the summing gearbox to reduce structural noise by designing, implementing, and making changes to the metal housing.



Figure 1. Special vehicle for oil exploitation.

There are many applications of the same nature and pursuing the same objectives for heavy vehicles. The main problem of this system is represented by the transmitted vibrations [1,2]. For example, in [3], considering heavy-duty construction equipment with increasing complexity, a major component of this equipment must be monitored. A failure among these components (gearbox, bearings, axles, and torque converter) may result in time lost with the machine standing until a repair is made. The critical driveline parts must be monitored to reduce the maintenance costs. To do this, sensor data for the gearbox, torque converter, axles, or bearing are used. The results of this paper show that the vibration properties of the studied components play a significant role in early fault detection of the driveline. It is important to identify the deviations from normal behavior.

Studying the vibrations of a gearbox, it is found that two types of vibrations are important, caused by two types of excitation sources, in the case of these parts of the vehicle. First are the internal excitation of the gears, and next the external excitation due to the input torque. A model to study the effects of this kind of excitation on the housing of the high-speed trains is presented in [4] using a multibody dynamic model. This model takes into account the elastic deformation of the wheel set and the gearbox housing. To do this, the soft MATLAB/Simulink is used. Experimental measurements confirm the accuracy of the model. The main result of the work is the highlighting of the effect that the traction torque has on the vibrations of the housing and on the amplification of the vibration acceleration. This can influence the calculus of the fatigue damage of the housing.

A gearbox used in a heavy truck generally is a massive aggregate having an important impact on the price of the truck as a whole. At the same time, some factors such as comfort and durability are determined by the vibration of the transmission. In [5], the study is dedicated to improving the design of a planetary gearbox by reducing its weight but at the same time having good behavior regarding vibrations and overload.

One type of gearbox widely used in practice is the Planetary Gearbox (PG), in commercial, industrial, or military applications. A dynamic model of the gearbox is proposed for the analysis of such a PG in order to achieve a reliable solution with excellent behavior and produced at a low-cost price in [6]. A two-step PG is analyzed. Interesting solutions are proposed to control the spread of trusts, in order to have a calculation method that provides some predictable results. Experiments were performed that demonstrate the usefulness of the presented dynamic model.

Vibration is one of the main causes of noise that is generated and transmitted by the gearbox [7]. For this reason, there have been numerous works that have dealt with the analysis of vibrations, both from an experimental point of view and from a theoretical point of view. Models were developed that were verified by experiments [8,9]. The equation of motion equations for dynamic analysis [10], the use of the finite element method [11,12], and the modeling of the mechanical system consisting of the gearbox [13] have been the subject of research in numerous papers, of which we have exemplified a few.

The use of the modal analysis is presented in [14,15], and the more sophisticated methods and the coupling of the vibrations that appear are presented in [16,17]. Another method of approach, using active control systems, is presented in [18,19], and a very detailed analysis of a deviate box with its specificities is presented in [20].

Although for the attenuation of the noise generated by the box, due to the gears, bearings, and frictions between the mechanisms inside the box, research has been done and continues to be done, for the noise of the box housing structure (structural noise), there are no multiple reduction possibilities. The main reason is economic and technological, because the reduction of structural noise is achieved by stiffening (addition of masses). This leads to considerable costs for materials and changes in manufacturing technology and assembly.

Therefore, it becomes particularly important to find a solution to improve the structure of the summing and distribution box so that it has as few vibrations of the external surfaces with as few constructive and technological changes as possible and at minimal material and financial cost.

The experimental evaluation of the radiated structural noise is of major importance, both in assessing the noise sources, but also in assessing the factors that, from the design phase, can be chosen to attenuate the noise of the adder and distribution box. To predict the noise radiated by the surfaces of the adder box based on the results obtained experimentally and to identify the parameters on which to act in order to structurally optimize the adder box, the paper presents a modal analysis performed with the finite element method.

The paper also presents a structural analysis performed with the finite element method, accompanied by the experimental determination of the characteristics of the housing material and its resistance limit in operation. These results may be useful in determining the importance of how parameters, such as structural attenuation, stiffness, and mass, influence structural noise.

The experimental method presented has been applied in the research of the structure of the housing of the adder box and can be extended to other components or structures of the vehicle that, being in a state of vibration, are sources of its noise. Thus, it can be applied to attenuate the noises generated by the auxiliary systems of the power group, the transmission units (gearbox, gears, Cardan shaft, and differential mechanism), the various housings, chassis, cab, body, and side walls of the platform. Consequently, the experimental method presented is particularly useful and has a wide field of applicability in the processes of attenuation of structural noise and implicitly of the noise generated by the vehicle.

It also presents the changes made to the structure of the box of the adder box, changes proposed and made following the analysis of the results obtained experimentally, as well as comparative tests on the two variants of the box (modified versus initial) to validate the changes and highlight improvements regarding the reduction of the structural noise of the CSD 4000 adder gearbox housing.

The paper determined experimentally the basic parameters of the vibration of the structure of the housing of the summing box (resonant frequencies, amplitudes of vibration displacements of the structure surface, and their distribution on the analyzed surface).

The authors' contribution consists of an improved project of a summing box, which ensures a lower level of vibrations (therefore also of noise) and a lower weight of the whole gearbox.

The paper will present the classic version of a summing box. Vibration measurements are made of this variant. Then, based on the measurements, an improved welded version of the metal housing is proposed. Measurements are then made that are, in the end, compared with the results obtained in the case of the classical variant. The main contribution is to propose a constructive variant that would allow the weight of the adder box to be reduced without affecting its noise level.

During the paper, the adder box was studied for a heavy machine, used in the oil industry. The results obtained are, first of all, valid for heavy vehicles. An extension of these results to other types of vehicles must be made carefully, mainly because different types of vehicles, for different activities, have individual structures that can be much different and, as a result, the generation and transmission of vibrations can be different. However, the methods can be used to study similar gearbox and transmission systems.

2. Presentation of the Adder Box

The adder box consists of a housing divided into compartments. The upper part of the housing is closed by the large cover, which is relatively rigid, and the lower part is closed by full sheet metal welding where we have the differential and the oil bath. Additionally, in the upper, middle, and lower parts of the housing, there are the covers that support the gears. Thus, the surfaces of the box as well as the large cover, although they have a relatively large thickness, have a reduced rigidity due to the presence of large holes through which the shafts with assembled gears must pass during assembly. The box is made of steel OLC37.3.

The overview is shown in Figure 2, where the notations have the following meanings:

- A. The input shafts, which receive the movement from the gearboxes of the power groups, by means of Cardan transmissions, have the possibility to engage or disengage the power groups according to the needs. On these shafts are mounted gimbal flanges to which the power groups and gears are coupled.
- B. Intermediate shafts I, which transmit the power flow to the power take-off shaft and drive two Parker type F1-51-L 378 1051 hydraulic pumps at the same time, which can be coupled as required.
- C. The shaft of the power take-off, which ensures the transmission of the power flow to the drilling rig and to the drive axles, by means of two gears provided with coupling mechanisms and the Cardan flange for driving the drilling rig. On the side opposite the drive flange of the unit, there is a pump with radial pistons ZF 8607.955.108., which ensures the lubrication of the box.
- D. Intermediate shaft II, which ensures, by means of a gear, the transmission of the power flow to the interaxial differential, driving at the same time the additional steering pump and the gear with crossed axes for the velocograph.
- E. The output shaft, which contains the interaxial differential, the drive toothed ring, the differential locking mechanism, and the Cardan flanges related to the Cardan transmissions to the chassis axles.

The technical characteristics of the adder box are:

- Maximum input moment: $2 \times 20,000$ Nm;
- Maximum input speed: 2100 rpm;
- Transmission ratio to shaft B: 1.275;
- Transmission ratio to shaft C: 1.4;
- Transmission ratio to shaft E: 1.1;
- Mass: approx. 1650 kg.

Considered as a truss, the housing structure is much more rigid when bending in the vertical transverse plane, perpendicular to the axis of the vehicle, than in the vertical longitudinal plane (containing the axis of the vehicle). Additionally, the excitation forces act perpendicular to the walls, thus constituting a major area of noise radiation. Thus, bending waves in the longitudinal vertical plane are the main causes of noise generation.



Figure 2. Adding box CSD 4000. (A) The input shafts; (B) Intermediate shafts I; (C) The shaft of the power take-off; (D) Intermediate shaft II; (E) The output shaft.

The adder and distribution box has a housing consisting of four plate-type elements, two assembled by welding with the third side-wall element, and the fourth (cover) assembled by screws. Figure 3 shows the assembled box housing.



Figure 3. Adder box housing before mounting the covers and gears.

The construction of a gearbox, distribution or summation and distribution, in this case, is conceived and designed primarily for the transmission of torque.

The forces in the gears inside the housing act on the outer housing and, through the shafts and bearings, produce bending forces that are felt by the housing. Therefore, the box housing will vibrate in response to its applied internal forces, and these structural vibrations will be transmitted through the structure to its outer surfaces and attached components, thus generating structural noise and, of course, airborne noise. Although the vibrations are of very small amplitudes, they will produce very large increases in the noise level.

The analysis of the noise transmission mechanism in the structure of the summing box housing by previous works (see Section 1) outlined the following conclusions:

1. The transmission of the vibrations produced in the structure is done mainly on the inner path, i.e., through gears in gears, bearings from the bearings, to the walls of the housing. This demonstrates why, especially in transmission units that transmit high moments (hence the case of the CSD 4000 adder gearbox), the importance of acoustic optimization of the housing structure is important in order to obtain a gear that has a low noise structure.
2. The vibratory properties of the components through which the vibrations are transmitted are decisive in their transmission. In current gearboxes or distribution boxes, which are mainly characterized by rigid connections between all their parts, virtually all internal components contribute to noise radiation.
3. The resulting noise will depend on the vibration properties of the parts that make up the structure of the adder box housing. Therefore, determining the vibration characteristics of the carcass structure is of major importance in determining the noise transmission mechanism.
4. Considered as a vertical beam, the structure of the housing of the adder box is much more rigid when bending in the vertical plane transverse to the longitudinal axis of the vehicle than in the vertical longitudinal plane to the longitudinal axis of the vehicle. Additionally, the excitation forces act perpendicularly on the walls of the housing, thus constituting a major area of noise radiation. Thus, the bending waves in the longitudinal vertical plane are the main causes of the generation of structural noise.
5. The study of the distribution of the structural noise on the surface of the box of the summing box is particularly useful in the design of structural measures. The highest vibrations occur in the power take-off area, between the walls of the main shaft bearings.

3. Structural Analysis of the Adder Box Housing

For all the experiments and analyses that will follow in this paper on the housing of the adder box, three points are established on the front surface of the housing and three points on the rear surface of the housing (considered in the normal mounting on the chassis). The points were chosen in the area of the two inputs in the box and in the area of the power take-off.

The coordinates of the measuring points, expressed in mm, on the two surfaces of the housing in the coordinate system considered for normal mounting on the chassis are given in Table 1.

Table 1. Coordinates of measuring points (x, z).

Front Surface of the Housing		
Point No. 1	Point No. 2	Point No. 3
(500, 1200) mm	(1200, 1200) mm	(850, 600) mm
Rear Surface of the Housing		
Point No. 4	Point No. 5	Point No. 6
(1200, 1200) mm	(500, 1200) mm	(850, 600) mm

3.1. Static Analysis of the Body of the Adder Gearbox

Body modeling consists of discretizing the solid into finite elements. Constraints are established by eliminating or restricting certain degrees of freedom for certain elements. The constraints actually reflect how the body is supported in reality or tend to reproduce it as accurately as possible. In Figure 4a,b the discretized model of the housing can be seen.

In the case of the adder gearbox housing, the ABAQUS program was used. Figure 5 shows the housing of the adder box with the stress field for the maximum load force along the axis of the shaft. It is observed that the maximum value of the effort is 8.82 N/mm² and it develops in the area of the power take-off of the box.

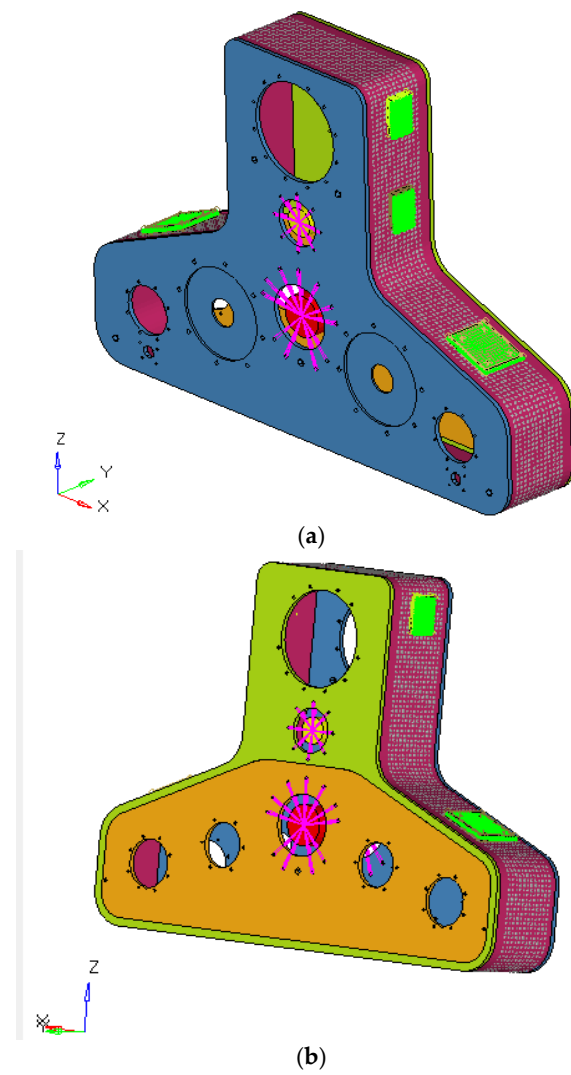


Figure 4. FEM model for the housing of adder gearbox. (a) Front housing; (b) rear housing.

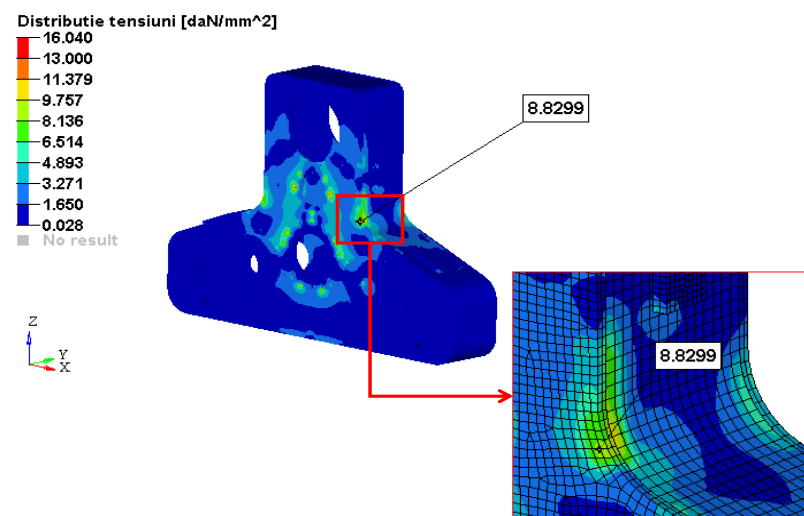


Figure 5. Stress field on the housing of the adder gearbox.

3.2. Modal Analysis of the Adder Gearbox

The modal analysis consists of finding the eigenmodes of vibration of a structure or of its parts (components), as well as the way in which these modes influence its constructive elements. Modern test methods can extend the frequency range, in the case of a modal analysis of a structure, by up to 3 kHz, recording the vibration modes highlighted by the elastic deformations of the structure at the time of maximum amplitude. Modal analysis is used to determine the eigenfrequencies and natural eigenmodes of vibration of an elastic system. The equation of motion for an undamped free system is expressed as:

$$[M] \{\ddot{u}\} + [k] \{u\} = \{0\} \tag{1}$$

where: $[M]$ is the mass matrix, $[k]$ the stiffness matrix, and $\{u\}$ the nodal displacement vector.

For a linear system a solution of the free vibrations will be harmonic of the type:

$$\{u\} = \{\phi\}_j \cos\omega_j t \tag{2}$$

where $\{\phi\}_j$ represents the eigenmodes, ω_j the eigenvalues, and t time.

In the case of the adder and distribution box housing with the ABAQUE program, 105 eigenmodes have been determined in the frequency range 100–2000 Hz. In Table 2, some of the obtained vibration modes are passed.

Table 2. Some of the calculated eigenfrequencies.

Frequency Areas (Hz)							
100–500		500–1000		1000–1500		1500–2000	
No. Mode	Frequency	No. Mode	Frequency	No. Mode	Frequency	No. Mode	Frequency
1	135	14	611	39	1019	76	1525
3	249	18	653	42	1063	79	1607
5	305	21	716	45	1126	82	1659
6	361	22	778	48	1150	85	1701
7	380	24	800	52	1200	88	1737
9	490	28	847	56	1244	91	1805
		33	904	60	1300	94	1834
		35	959	65	1355	97	1896
		38	1000	68	1412	98	1901
				70	1453	102	1936
				74	1498	103	1976
						104	1980
						105	1984

It is observed that as the frequency increases, the number of vibration modes increases. Figures 6 and 7 show modes 1 and 7 in the 100–500 Hz frequency range.

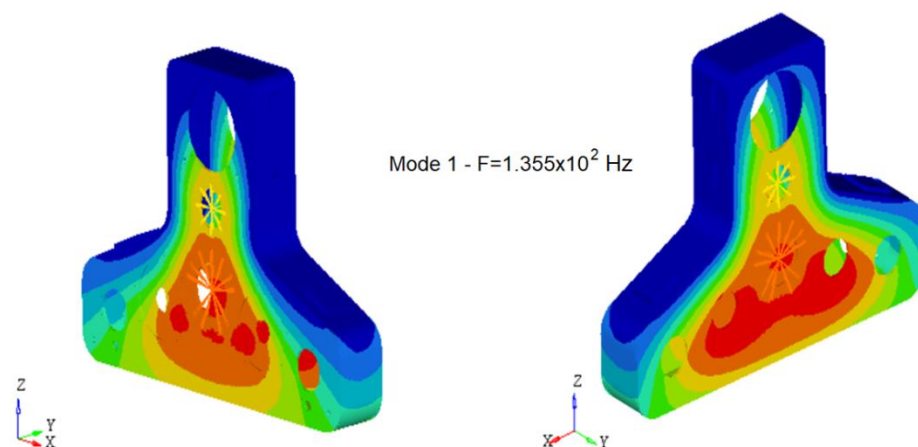


Figure 6. Eigenmode 1 (frequency—135.51 Hz).

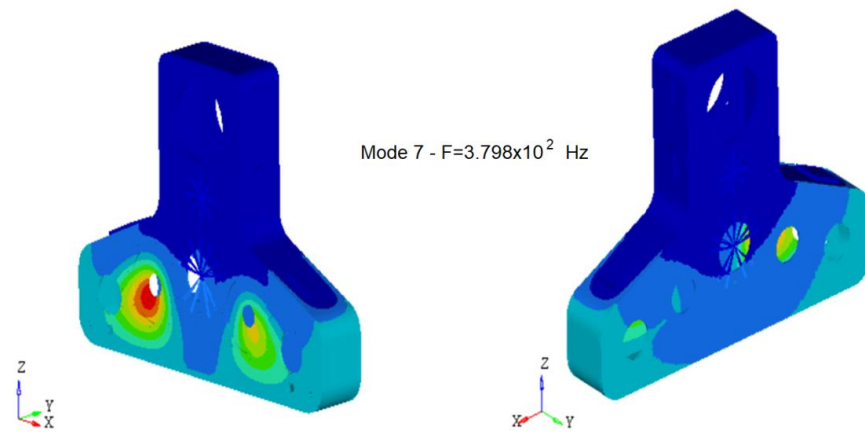


Figure 7. Eigenmode mode 7 (frequency—379.89 Hz).

It is observed that the areas most excited and vulnerable to excitation are those around the power take-off with propagation tendencies toward the differential area. The images show the distributions on both the front and the back surface of the box.

From Figure 7, we can distinguish the restriction of vibrations towards the upper area of the housing, an area sensitive to low frequencies. Figures 8 and 9 show modes 22 and 76 in the 500–2000 Hz frequency range.

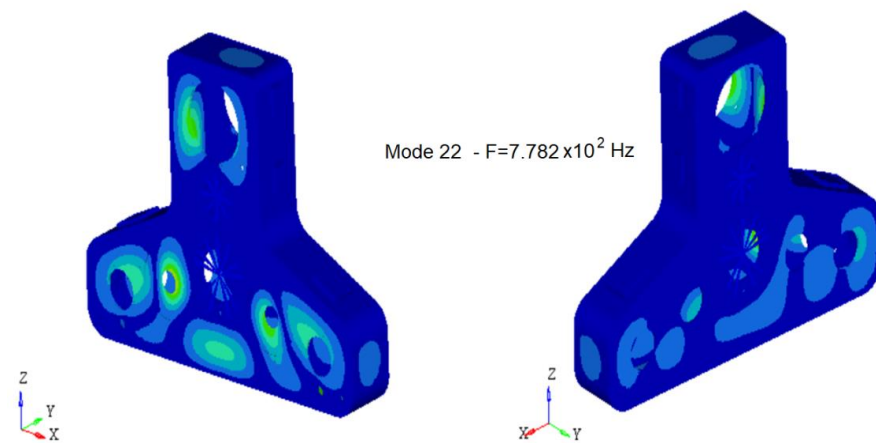


Figure 8. Eigenmode 22 (frequency—78.28 Hz).

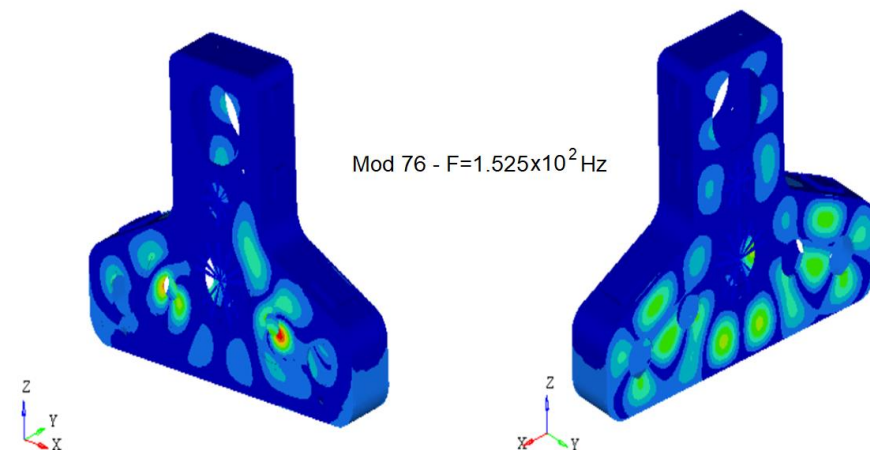


Figure 9. Eigenmode 76 (frequency—1525.78 Hz).

Figure 10 shows the distribution of displacements on the front surface of the housing at an excitation with the frequency of vibration mode 1. Figure 11 shows the distribution of displacements in the three measuring points on the rear surface of the housing at vibration mode 1 (135.51 Hz). The largest displacements are in the power take-off area.

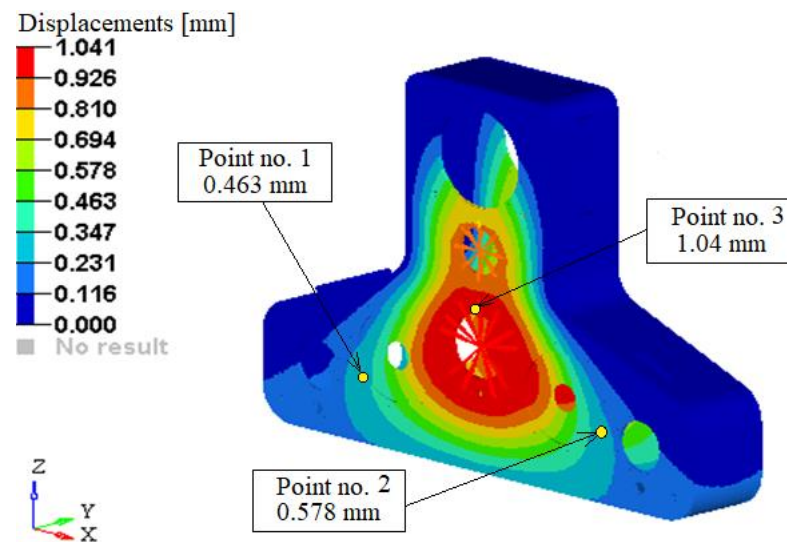


Figure 10. Distribution of the displacements on the front surface of the housing.

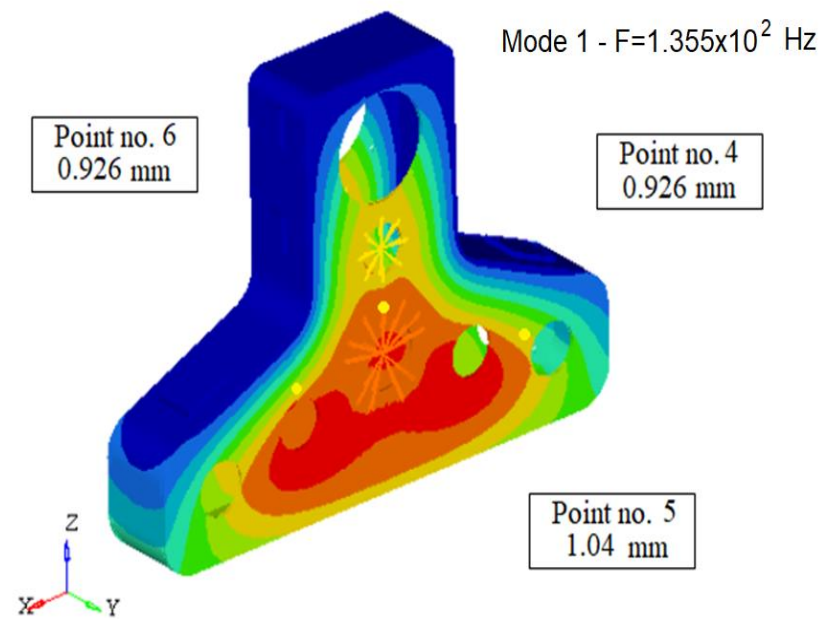


Figure 11. Distribution of the displacements on the rear surface of the housing.

Figure 12 shows the displacements in the measuring points on the front surface of the housing for vibration mode 7 (379.89 Hz), and Figure 13 shows the displacements in the measuring points on the rear surface of the housing.

Figure 14 shows the displacements in the measuring points on the front surface of the housing for vibration mode 76 (1525.68 Hz), and Figure 15 shows the displacements in the measuring points on the rear surface of the housing for vibration mode 76 (1525.68 Hz).

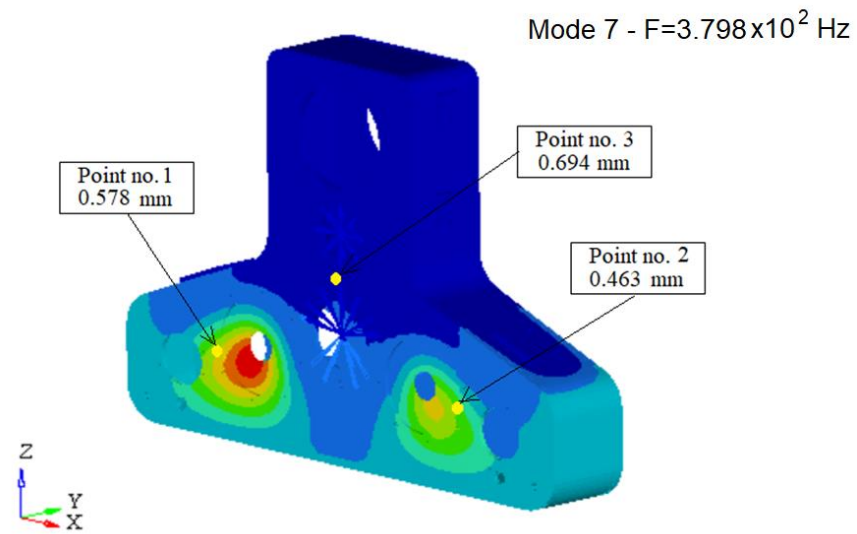


Figure 12. Displacements at the points on the front surface of the housing for mode 7.

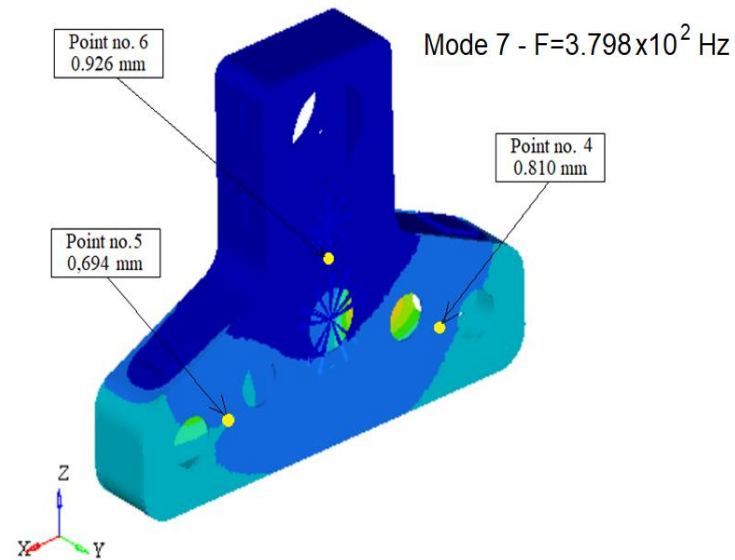


Figure 13. Displacements at the points on the rear surface of the housing for mode 7.

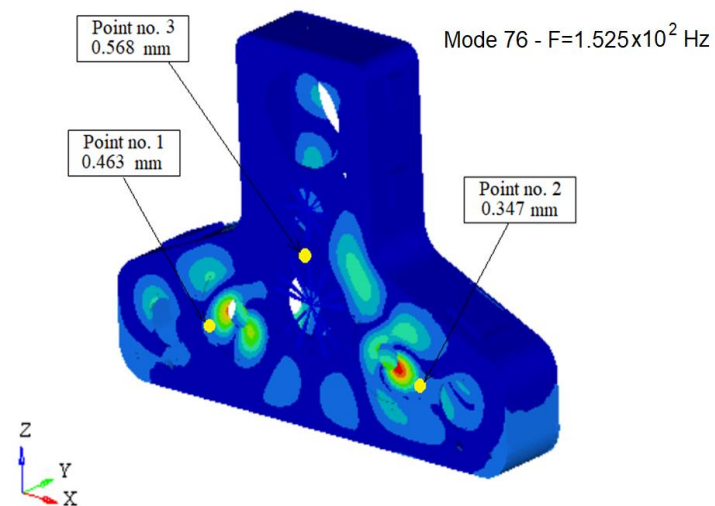


Figure 14. Displacements of the points on the front surface of the housing for mode 76.

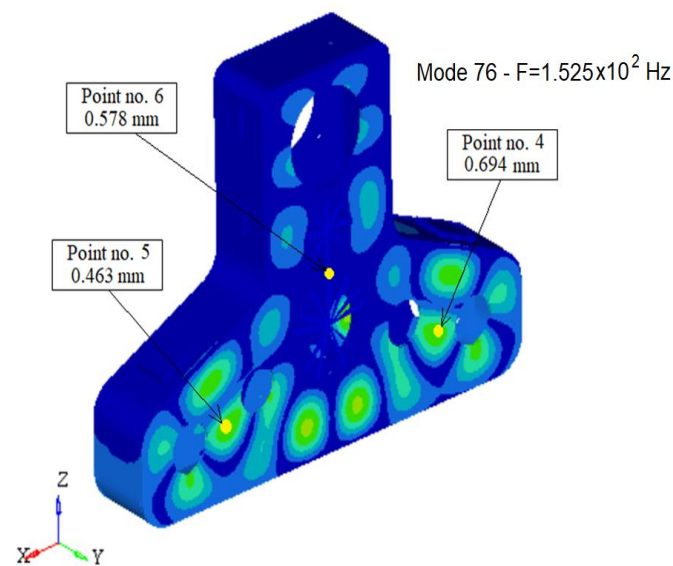


Figure 15. Displacements of the points on the rear surface of the housing for mode 76.

In this section, the structural and modal analysis of the adder and distribution box housing was performed with the finite element method using the ABAQUS program and experimental determinations of the housing material characteristics. In conclusion, we can highlight the following aspects:

1. The structural analysis highlighted the distribution of unitary efforts on the surfaces of the box housing.
2. For the maximum load of the box (maximum transmitted moment), the greatest efforts are distributed in the power take-off area.
3. The highest value of the effort is 88.229 N/mm^2 in the area of the large cover assembled by screws, close to the left side edge.
4. The housing material is OL37.3 and has an operating resistance limit or unlimited fatigue strength (in the case of the carcass, which is made of welded elements) of maximum 13 daN/mm^2 .
5. The maximum stresses in the material of the adder box housing must not exceed the unlimited fatigue strength estimated at 13 daN/mm^2 for the material OL37.3.
6. The modal analysis determined 105 eigenmodes of vibration in the frequency range from 30 to 2000 Hz.
7. In the field of low frequencies, the housing has fewer modes of vibration, but the amplitudes of vibration are higher at low frequencies.

In conclusion, the housing of the adder box must be stiffer in order not to generate high structural noise.

3.3. Experimental Tests

In order to improve the constructive solution of the summing and distribution box through structural measures, it is absolutely necessary to establish the criteria by which to predict, from the design phase, the vibration characteristics and the noise level radiated by the individual box structures, especially the housing structure. Their knowledge gives the possibility to use the finite element method (FEM) in the design phase, so as to be able to reduce the total mass of the box as well as the costs related to materials, technology, and labor.

This chapter presents an experimental, efficient, useful, and fast method to determine:

- The eigenfrequencies of the structure of the housing of the adder gearbox to which correspond maximum values of the noise radiated by its surfaces.
- Radiated noise from the housing surfaces.

- The amplitudes of the vibration displacements of the surfaces of the box structure of the adder gearbox and their distribution on the analyzed surface.

The experimental results obtained constitute major information necessary to determine the characteristics of structural noise transmission as well as the stresses in the housing.

The results obtained from the experiments performed on a housing in the composition of the CSD 4000 adder gearbox are presented.

The experimental research program consists of:

- Experimental analysis of eigenfrequencies.
- Measurement and experimental analysis of the noise radiated by the housing surfaces.
- Determination of the eigenfrequencies to which correspond maximum values of noise radiated by the housing surfaces.
- Measurement of vibration displacements of the housing surfaces.
- Comparison of the values of the amplitudes of the vibrations of the housing surfaces obtained by simulation in Section 3.3, with the measured values.

To perform the experiments, the housing structure of the adder gearbox was brought into a state of simulated vibration. Additionally, because the housing structure is much more rigid when bending in the vertical plane (parallel to the front and rear surfaces of the housing) than in the horizontal plane, the bending waves in the horizontal plane being the main causes of structural noise transmission, housing excitation was performed horizontally using an electrodynamic exciter.

The adder and distribution box is mounted on the chassis by means of screw supports, their rigidity being very high (the rubber used has high rigidity). To simulate these conditions, the analyzed housing was mounted with its mounting brackets, which are fixed on two brackets mounted on the laboratory platform, brackets that practically simulate the vehicle chassis.

The experimental analysis of the vibration behavior of the box housing structure was performed by bringing it into a simulated vibration state in the frequency range 30 Hz–2000 Hz.

If the experimental analysis of the vibration behavior of the gearbox housing structure was performed by conventional methods, using many acceleration transducers, the following specific difficulties would arise:

- A large number of measuring points would be needed.
- The number of measurements performed simultaneously would be restricted by the capacity of the available equipment, which must ensure the simultaneous transfer of the measured values. Additionally, in order to establish the relationships between the phases, it would be necessary that the measurements be performed against a reference quantity.
- It would not be possible to specify how many measuring points need to be analyzed, because it would be impossible to fully describe all the details of the vibration modes.

The detail presented in Figure 16 shows:

- An electrodynamic exciter.
- An impedance transducer.
- Adder gearbox housing.

The accelerator transducer was mounted next to the force transducer. The vibration of the gearbox housing structure is taken over by the acceleration transducer, which it transforms into an electrical signal proportional to its acceleration. Thus, the impedance transducer (Kaman, Middletown, OH, USA) will have two outputs, one providing a signal proportional to the acceleration and the other providing a signal proportional to the force. The vibration measuring system was calibrated using an electrodynamic calibrator type 11 032 (Siemens, Munich, Germany) by the absolute calibration method with an accuracy of $\pm 5\%$. The force signal is amplified by means of a KWS 3082 HOTTINGER measuring amplifier (Hottinger Brüel & Kjaer GmbH, Darmstadt, Germany), whose deviation from linearity is less than 0.05%, and then applied to the input of the FFT (fast Fourier transform) frequency analyzer.

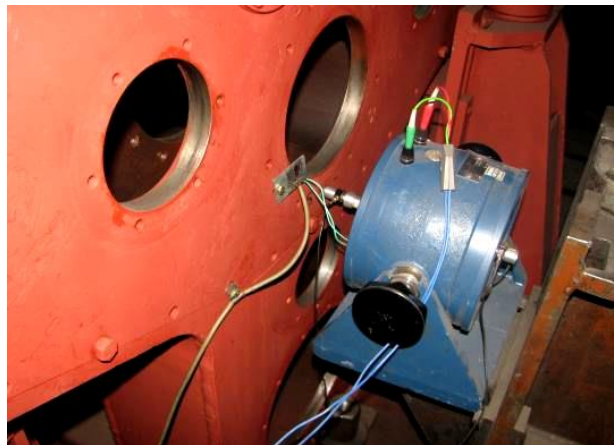


Figure 16. Detail of the vibration measurement and analysis installation.

The phase difference between the force and velocity vectors is visualized at the outputs of the two measuring amplifiers using a two-channel oscilloscope.

In order to perform the measurements and analysis of the vibrations of the structure of the housing of the adder box under simulated operating conditions (obtaining a state of vibration thereof), the housing was excited by means of an excitation installation. The signal regulator module has the role of comparing the size of the control signal received from the signal generator with the size of the “feedback”-type control signal received from the impedance transducer. The frequency scanning module has the role of varying exponentially in a round-trip cycle the frequency of the excitation signal between two limits, maximum and minimum, set by the operator, with an adjustable scanning speed. The obtained excitation signal is amplified by means of the power amplifier and then transmitted to the electrodynamic exciter. The analysis of the signal obtained from the force measuring amplifier, which is directly proportional to the numerical value of the point mechanical impedance, was performed in the frequency domain. This analysis decomposes the complex signal into components corresponding to various frequencies.

The frequency domain analysis performed by calculating the power spectral density, which was used, is indicated for the analysis of random signals. The power spectral density was obtained by a real-time analysis using the FFT Fourier transform algorithm. Elimination of noise (electronic) and other parasitic components is achieved through a synchronous mediation, also called linear mediation in time, because it is commonly applied in the time domain. Linear time mediation requires the existence of a trigger synchronized with the system from which the signal is collected, which allows obtaining in the time domain several synchronized signal sequences, which are mediated before performing the transformation. Through mediation, asynchronous parasitic signals will be greatly attenuated or even canceled if the number of sequences is large enough.

The analysis of the obtained signals was performed with the help of the FFT frequency analyzer with the following technical characteristics:

- Frequency response sensitivity: ± 0.2 dB (with antialiasing filtering).
- Number of spectral lines: 400.
- Linear mediation: for a number of 2048 mediations, the relative error of the obtained power spectral density is 1.1% or 0.1 dB.

In order to perform the measurements and analysis of the vibrations of the box housing structure in a simulated vibration state, excitation force having the following parameters was required:

- Signal shape: sinusoidal.
- Constant velocity: $v_{ex} = 4.10^{-3}$ m/s (rms value).

- Exponential back and forth variation of the excitation signal frequency with the speed of 1 oct/min, in two domains: 30 Hz–500 Hz with the resolution 1.25 Hz, and 300 Hz–2000 Hz with the resolution: 5 Hz.

The spectral power densities, linearly averaged, of the point mechanical impedance at three points located on the front surface of the housing and on the rear surface of the housing (considered in the normal mounting on the chassis) were determined experimentally. The points were chosen in the area of the two inputs in the box and in the area of the power take-off. The coordinates of the measuring points, expressed in mm, on the two surfaces of the housing in the coordinate system considered for normal mounting on the chassis are the same as in the previous point.

More results obtained in the experiments are presented in the Appendix A.

The amplitudes of the displacements on the rear surface of the carcass in the simulated vibration state were measured at two resonant frequencies determined experimentally using the technique of measuring the point mechanical impedance.

The measurements were made using the accelerator transducer. In order to obtain a signal proportional to the Y displacement, the signal coming from the accelerator transducer (Hottinger Brüel & Kjaer GmbH, Darmstadt, Germany), applied on the rear surface of the housing in the power take-off area, is integrated twice with the help of the integrating amplifier type 00 028 included in the vibration measuring equipment type 00 033.

The measured values (rms values) were read at the 1×10^{-3} mm accuracy of the vibration measuring equipment.

In order to obtain the vibration of the box housing structure and to perform the measurements of its surface displacements, the box housing was requested with an applied excitation force, in the area of the power take-off on the front surface of the housing, having the following parameters:

- Signal shape: rectangular.
- Constant speed: $v_{ex} = 4 \cdot 10^{-3}$ m/s (rms value).
- At two fixed resonance frequencies of the rear surface of the housing, determined experimentally using the mechanical impedance measurement technique: $f_1 = 395$ Hz and $f_2 = 1550$ Hz.

The measurement of the amplitudes of the vibration displacements of the box housing structure was performed with the help of the acceleration transducer in the measurement points No. 4, 5, and 6 on the rear surface of the housing, as opposed to the one on which the excitation force was applied.

Following the experiment, the amplitudes of the Y displacements of the back surface vibration of the box housing were obtained to compare with the displacements obtained by computer simulation according to the analysis by the finite element method presented in Section 3. The values of vibration displacement amplitudes at the points on the analyzed surface in Table 3.

Table 3. Measured displacements amplitude at points 4, 5, and 6.

Frequency (Hz)	Displacements Amplitude Y (mm)		
	Point No.4	Point No.5	Point No.6
395	0.55–0.75	0.60–0.70	0.85–0.95
1550	0.45–0.55	0.35–0.45	0.50–0.65

It is found that the highest vibrations occur in the power take-off area on the rear surface of the housing on the large cover mounted with housing screws.

3.4. Measurement of Displacements on the Front Surface of the Housing

The amplitudes of the displacements on the front surface of the housing in the simulated vibration state were measured at two resonant frequencies determined experimentally using the technique of measuring the point mechanical impedance.

In order to obtain the vibration of the box housing structure and to perform the measurements of its surface displacements, the box housing was excited with a force applied in the area of the power take-off on the rear surface of the housing, having the following parameters:

- Signal shape: rectangular.
- Constant speed: $v_{ex} = 4 \cdot 10^{-3}$ m/s.
- At two fixed resonant frequencies of the front surface of the housing, determined experimentally using the mechanical impedance measurement technique: $f_1 = 395$ Hz and $f_2 = 1525$ Hz.

The measurement of the amplitudes of the vibration displacements of the box housing structure was performed with the help of the acceleration transducer in the measurement points No. 1, 2, and 3 on the front surface of the housing, as opposed to the one on which the excitation force was applied

Following the experiment, the amplitudes of the Y displacements of the vibration of the front surface of the box housing were obtained for comparison with the displacements obtained by computer simulation according to the analysis by the finite element method previously presented. The amplitude values of vibration displacements at the points on the analyzed surface are presented in Table 4.

Table 4. Measured displacements amplitude at the points 1, 2, and 3.

Frequency [Hz]	Displacements Amplitude Y [mm]		
	Point No. 1	Point No.2	Point No.3
395	0.40–0.55	0.45–0.65	0.55–0.70
1550	0.25–0.40	0.30–0.40	0.45–0.55

It is found that the highest vibrations occur in the area of the power take-off on the front surface of the housing.

3.5. Comparison of the Values of the Vibration Displacements of the Surfaces of the Adder Box Housing Obtained by Simulation with the Experimentally Measured Values

In order to evaluate the accuracy of the analytical prediction (computer simulation by the finite element method) of the displacement values in the measuring points on the housing, they must be compared with the values determined experimentally.

The comparison of the values of the displacements in the measurement points on the housing, obtained by simulation, at the two chosen excitation frequencies, with the values obtained experimentally is presented in Table 5.

Table 5. Comparison of the measured and calculated values for displacements.

Frequency	Measurement Point	Displacements Amplitude (mm)	
		Simulation	Measurement
395	1	0.578	0.40–0.55
	2	0.463	0.45–0.65
	3	0.694	0.55–0.70
	4	0.810	0.55–0.75
	5	0.694	0.60–0.70
	6	0.926	0.85–0.95
1550	1	0.463	0.25–0.40
	2	0.347	0.30–0.40
	3	0.568	0.55–0.70
	4	0.694	0.45–0.55
	5	0.463	0.35–0.45
	6	0.578	0.50–0.65

There is a very good correlation between the values of the displacements determined analytically by running the ABAQUS program and the values of the experimentally determined displacements. From the analysis of the results obtained after performing the presented experiments, the following can be summarized:

5.1 Analysis of the vibration behavior of the structure of the adder box housing.

The structure of the analyzed box housing shows resonant frequencies approximately in the range of 390 Hz–2000 Hz with a dominant frequency of 395 Hz.

5.2 Measurement of the amplitudes of the displacements on the surfaces of the adder box housing.

- The highest vibrations occur in the area of the input shaft bearings and in the area of the power take-off bearings.
- The results obtained confirm that in the area of the cover mounted by screws (i.e., the upper part of the housing), the housing of the box has the lowest rigidity.
- There is a very good correlation between the values of the displacements determined analytically by running the ABAQUS program and the values of the experimentally determined displacements.

Finally, it can be stated that, by applying the experimental method presented in the process of optimizing the case of the adder box through structural measures, the following facilities are obtained:

- There is the possibility to determine without difficulty and with sufficient precision the resonance frequencies corresponding to the important vibration modes, generating structural noise radiated by the carcass surfaces.
- Resonant frequencies and maximums of the radiated noise spectrum can be predicted from the design stage with a maximum accuracy of only a few dB.
- Although the application of this experimental method does not require special conditions, and the measurement and analysis equipment does not involve a particular complexity, it still provides the necessary accuracy required by the structural acoustic optimization.

4. Analysis of Results and Presentation of Constructive Modification Solutions for the Adder and Distribution Box Housing

The obtained results highlight the important structural deficiencies of the summing box housing analyzed, especially for the rear surface of the housing in the area of the large cover mounted by screws. The following constructive modifications are proposed for the stiffening of the adder box housing:

- Removal of the large cover mounted by screws.
- Replacing the cover with welded housing plate.
- Inserting inside the housing and mounting by welding two tie rods (reinforcement) between the front surface and the rear surface of the housing in the area of the power take-off.
- Mounting by welding inside, on the side surfaces, front and back, six reinforcing ribs (three on the left and three on the right).
- Cutting and making three manhole covers at the top of the casing necessary for mounting the gears and the wheelhouse of the adder box.

In order to make these changes, the proposed parts were designed (Figures 17 and 18), the corresponding documentation was prepared, the parts were physically made, and a new adder and distribution box housing was installed.



Figure 17. New adder box, welded version.



Figure 18. New adder box with reinforcements.

5. Measurement and Comparative Experimental Analysis of the Vibrations in the Housing of the Adder Gearboxes

Based on the above analysis, an improved housing version was designed and made. In this chapter, we will present comparative experiments performed on the two adder gearboxes that we will call the old adder box, for the box equipped with the existing case, and the new adder box, for the box equipped with the improved case. All tests performed on the stand for the old adder box were also performed on the new adder box. It should be noted that the comparative experiments on the two summation boxes were performed under the same test conditions.

The comparative tests performed on the two summation boxes were the following:

- Measurements of accelerations, speeds, and displacements in the 6 measuring points on the housing established and presented in Section 4 (Figure 19).
- Measurements of radiated noise from the box one meter away from the four sides of the box.

The experimental analysis of the vibration behavior of the adder boxes in the initial version and the modified version was performed during the run-in program in idle (without load) on the test and testing stand. Figure 20 shows the two variants of adder boxes mounted on the test stand.



Figure 19. Acceleration transducer mounted at point No. 2 and 3 measures. Accelerometers are highlight with a yellow circle.

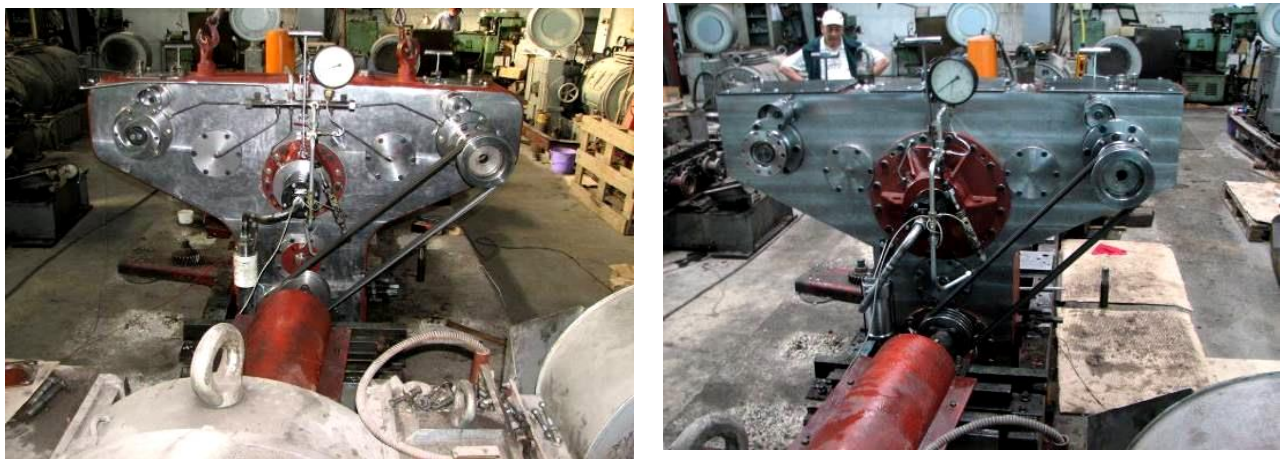


Figure 20. Old and new adder and distribution box mounted on the stand.

The measurements were made using an accelerator transducer. To obtain a signal proportional to the Y displacement, the signal coming from the accelerator transducer KD 35, applied in one of the points on the rear or front surface of the housing, is integrated twice with the help of the integrating amplifier type 00 028 included in the vibration measurement type 00 033 and integrated once to obtain a signal proportional to speed V and proportional to acceleration a. The amplitudes of displacements, velocities, and accelerations on the rear and front surface of the gearbox were measured in the six measuring points, in drive, at four test modes of 500, 1000, 1500, and 2000 rotations per minute, respectively. For displacements, the measured values were read on the vibration measuring equipment with an accuracy of 5×10^{-3} mm.

In Figures 21–23 are presented comparatively the evolution diagrams of the accelerations, in the 6 measurement points, for the 4 speed regimes, on the two adder boxes.

In Figures 24–26 are presented comparatively the diagrams of the evolution of the speeds, in the 6 measuring points, for the 4 speed regimes, on the two adder boxes.

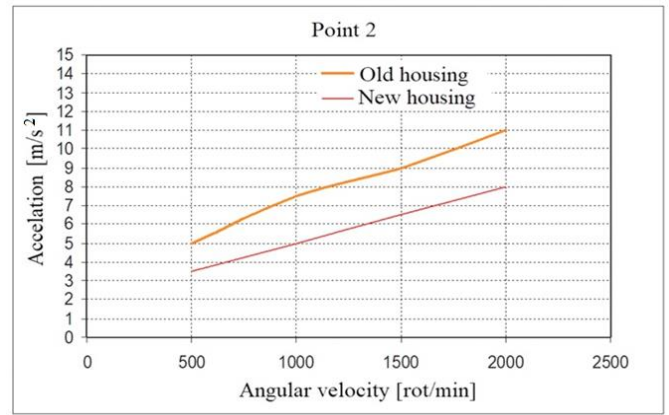
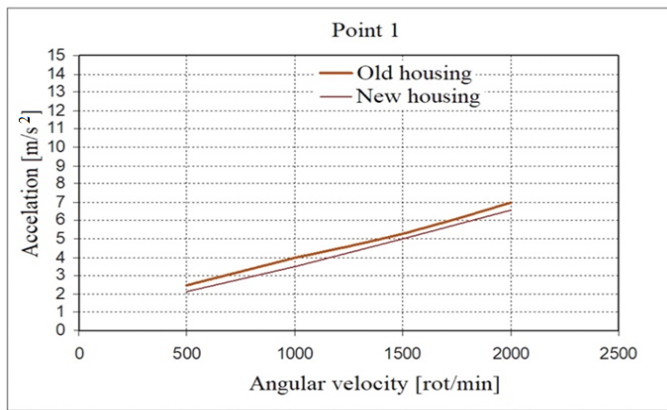


Figure 21. Measured accelerations at points 1 and 2 for the two versions (old and new).

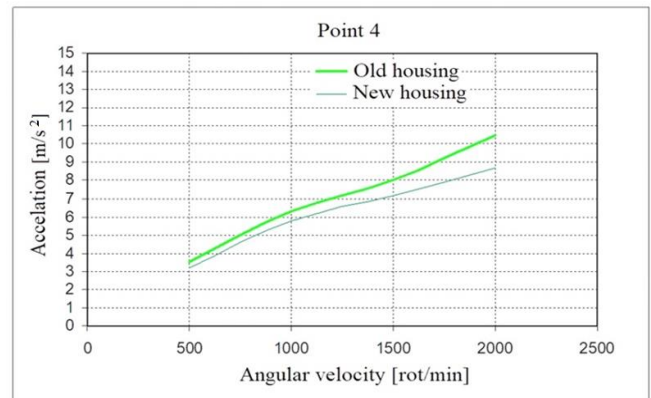
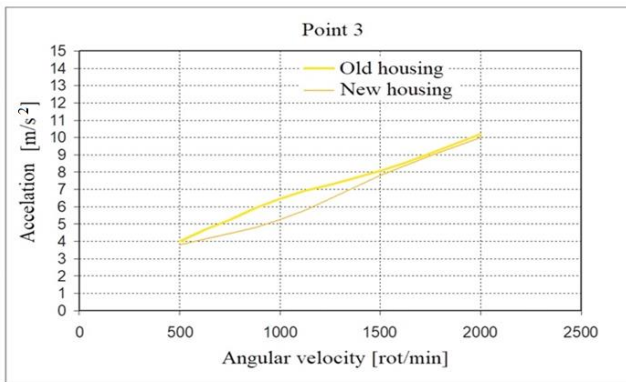


Figure 22. Measured accelerations at points 3 and 4 for the two versions (old and new).

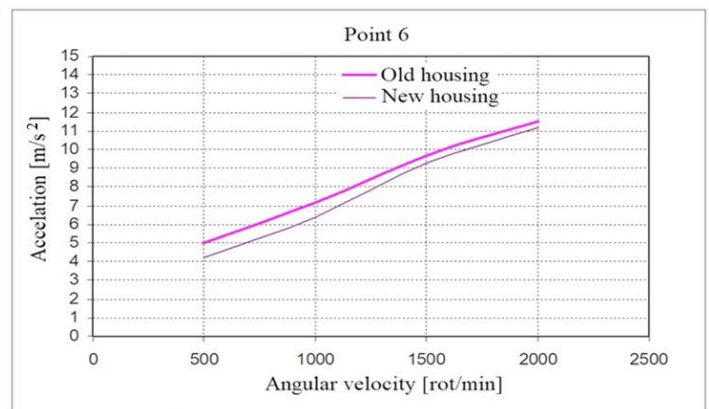
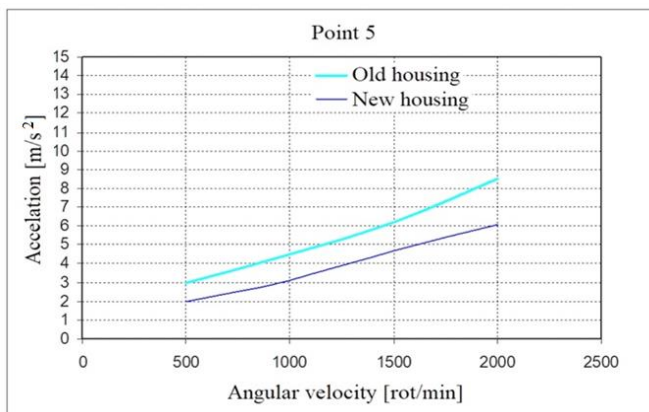


Figure 23. Measured accelerations at points 5 and 6 for the two versions (old and new).

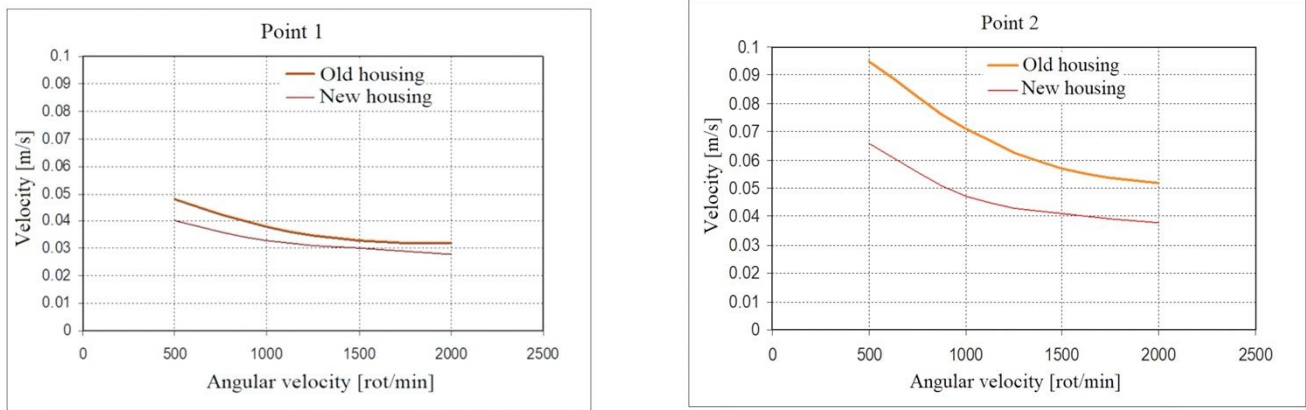


Figure 24. The velocities determined at points 1 and 2 of the two adder boxes (old and new version).

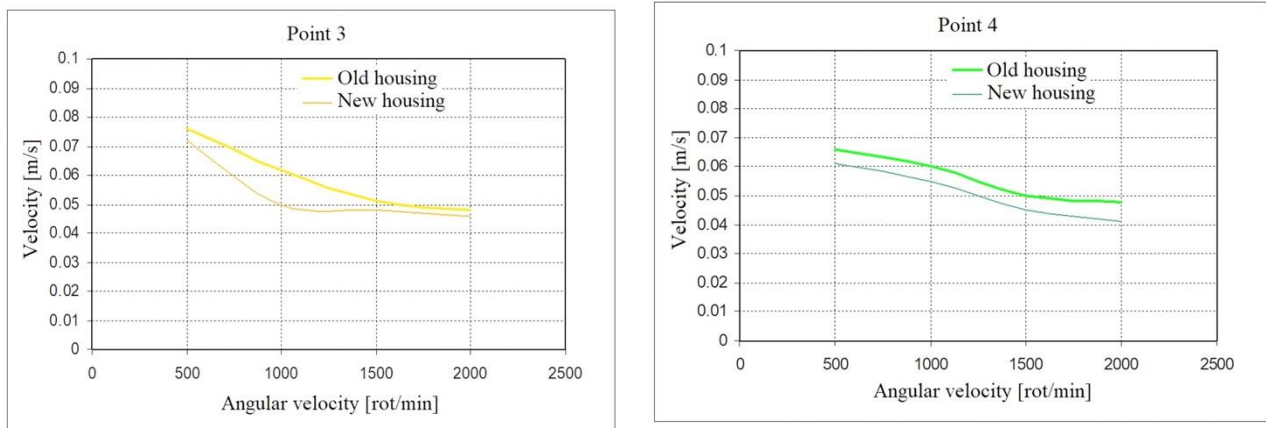


Figure 25. The velocities determined at points 3 and 4 of the two adder boxes (old and new version).

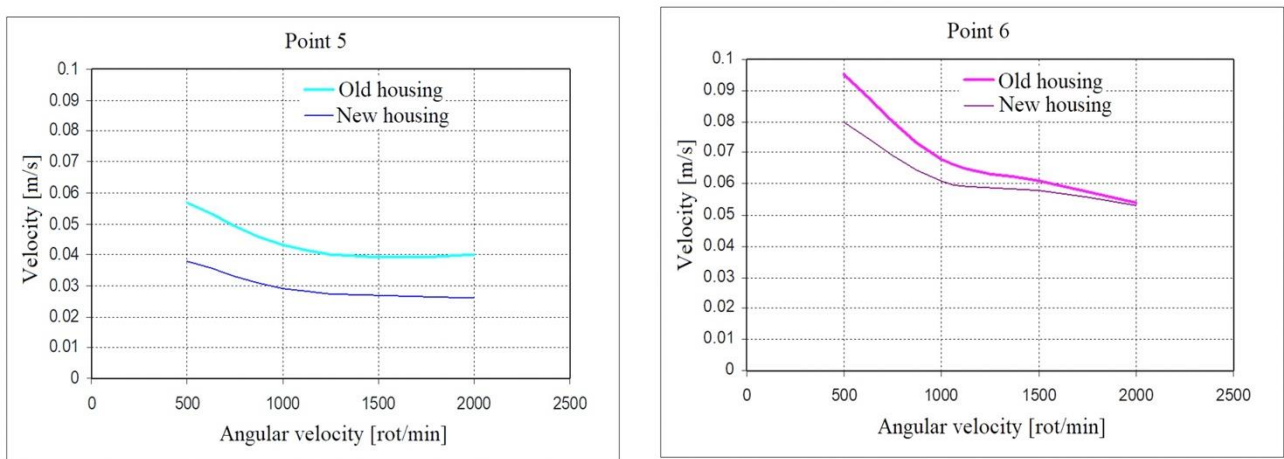


Figure 26. The velocities determined at points 5 and 6 of the two adder boxes (old and new version).

In Figures 27–29 are presented comparatively the evolution diagrams of the displacements, in the 6 measuring points, for the 4 speed regimes, on the two adder gearboxes.

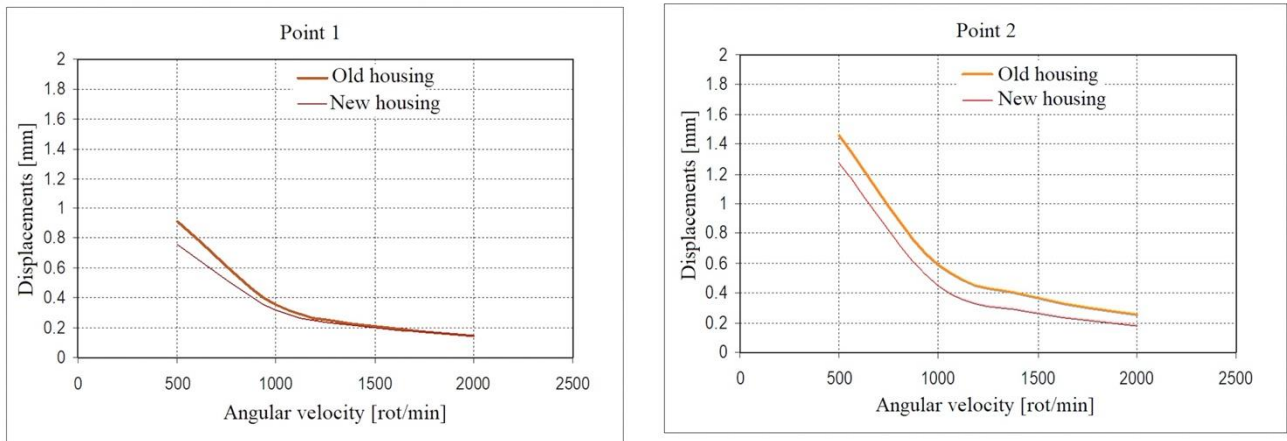


Figure 27. Displacements in measuring points 1 and 2 on the two summing boxes (old and new version).

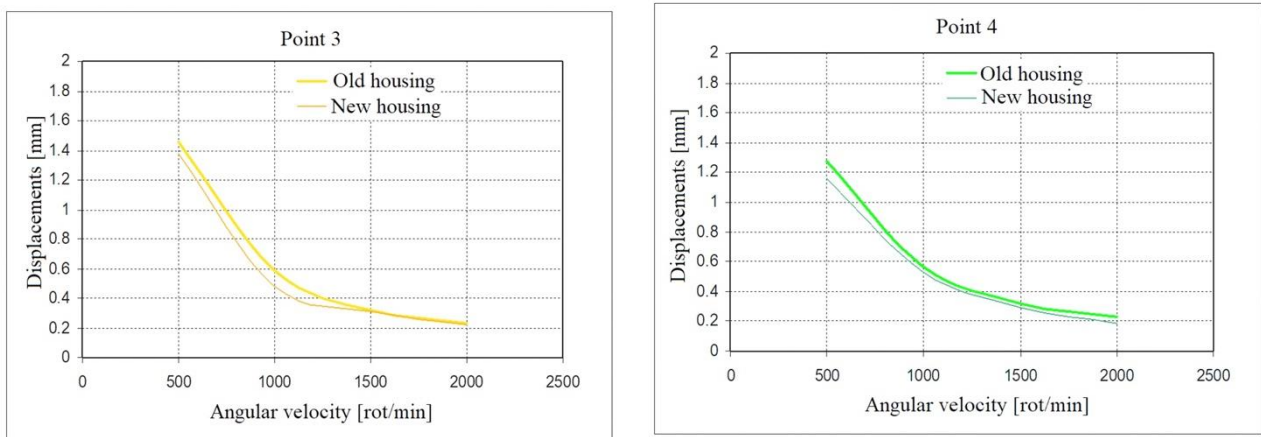


Figure 28. Displacements in measuring points 3 and 4 on the two summing boxes (old and new version).

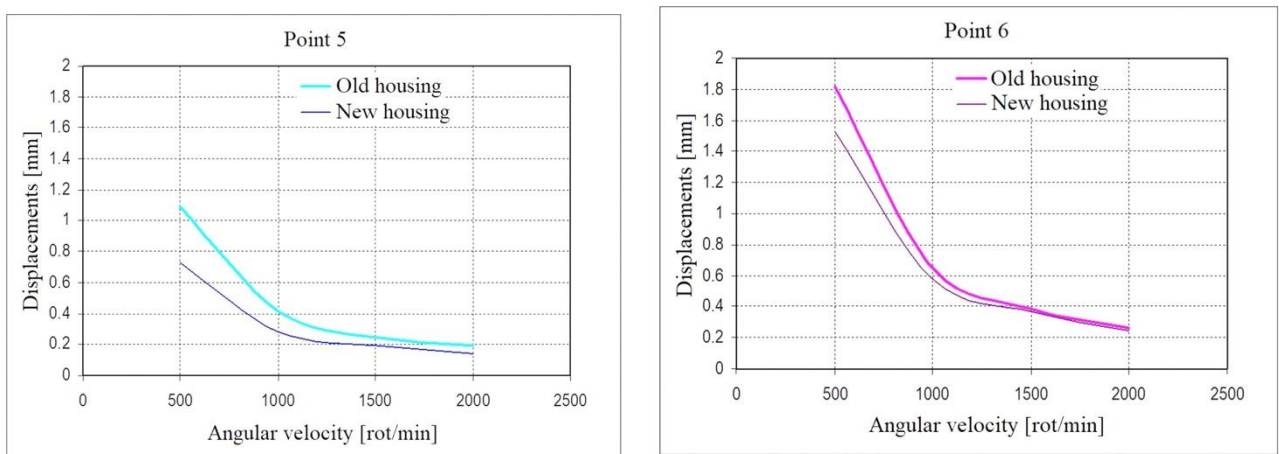


Figure 29. Displacements in measuring points 5 and 6 on the two summing boxes (old and new version).

The measurement and experimental analysis of the radiated noise (sound pressure level) from the surfaces of the adder and distribution boxes in the initial version and the modified version were performed during the run-in program at idle (no load) on the test stand.

6. Results

For the old and new adder box, for comparison, Figures 30 and 31 present the spectra of the sound pressure level radiated from the front surface, Figures 32 and 33 present the spectra of the sound pressure level radiated from the rear surface, Figures 34 and 35 present the spectra of the sound pressure level radiated by the left lateral surface, and Figures 36 and 37 present the spectra of the sound pressure level radiated by the right lateral surface.

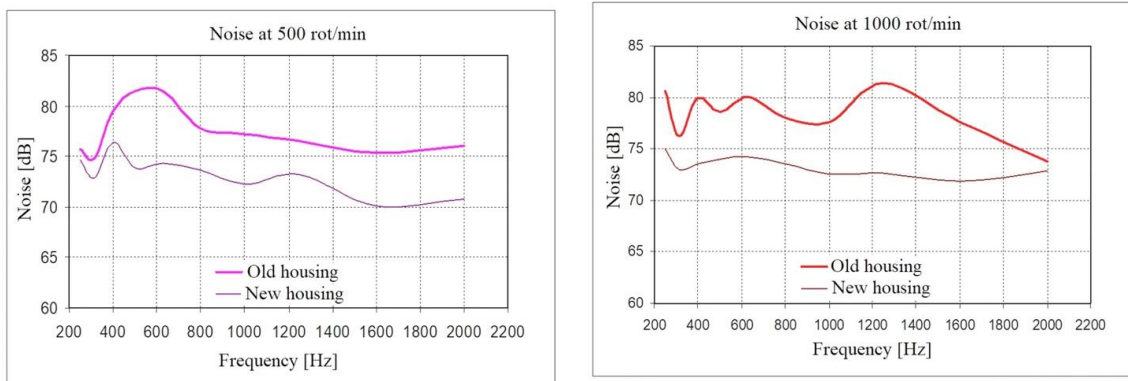


Figure 30. Lp sound pressure level diagrams for front surface at 500 and 1000 rpm.

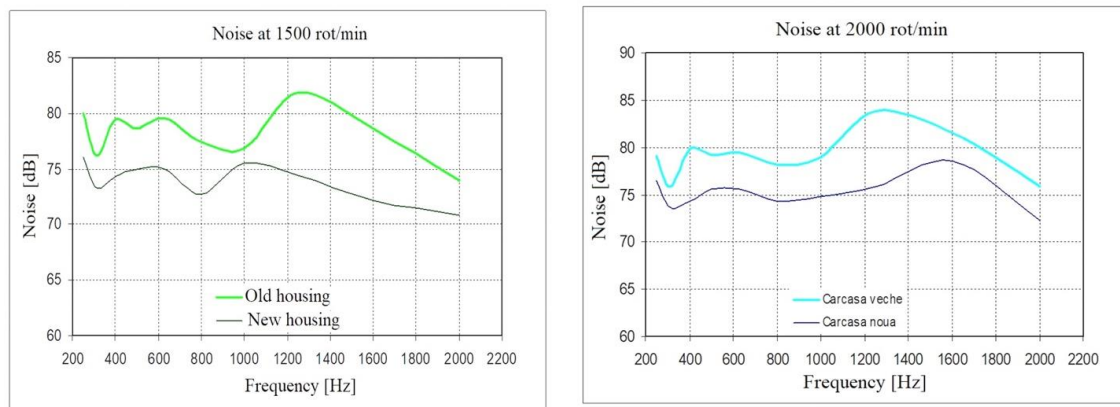


Figure 31. Lp sound pressure level diagrams for front surface at 1500 and 2000 rpm.

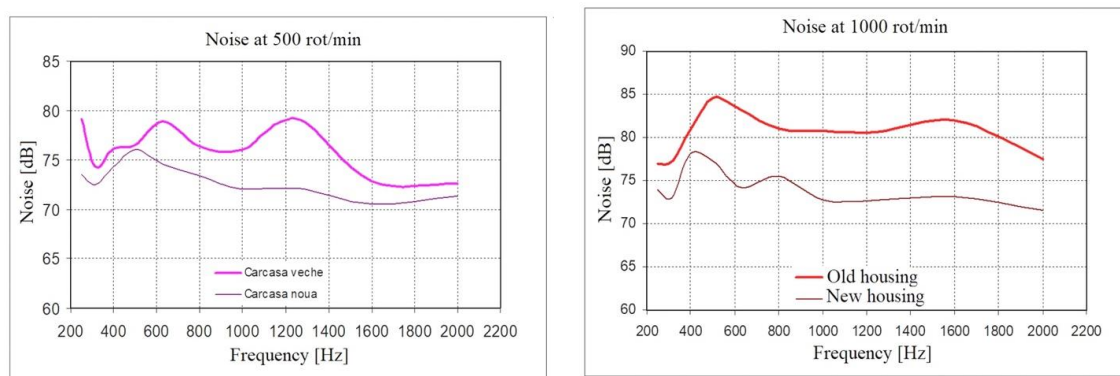


Figure 32. Lp sound pressure level diagrams for rear surface at 500 and 1000 rpm.

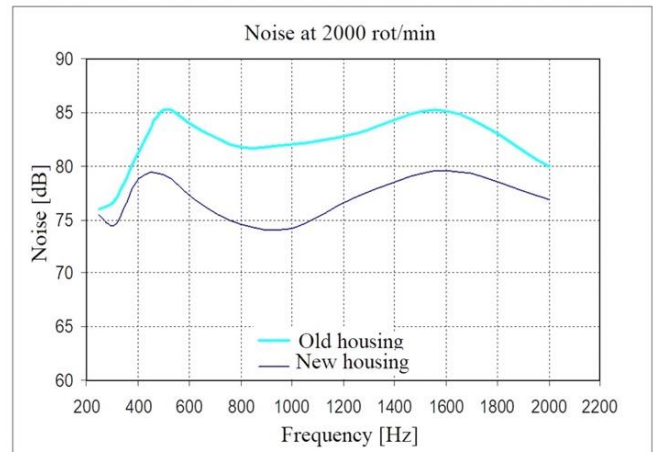
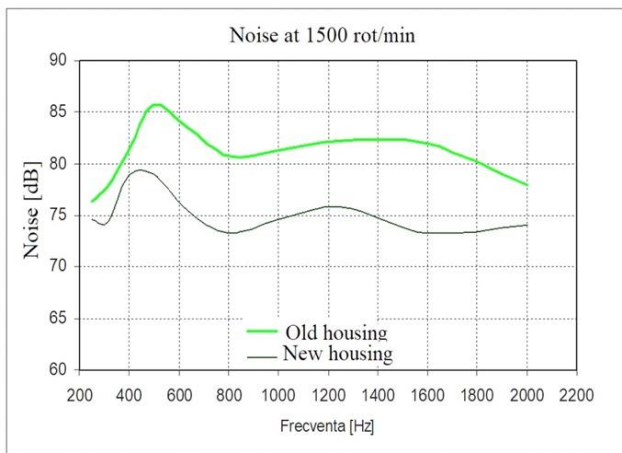


Figure 33. Lp sound pressure level diagrams for rear surface at 1500 and 2000 rpm.

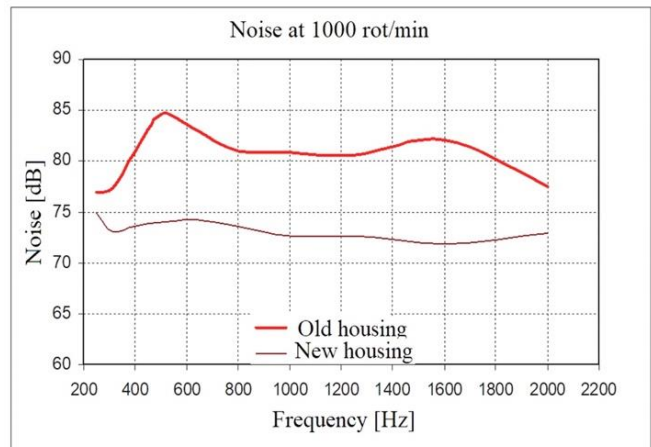
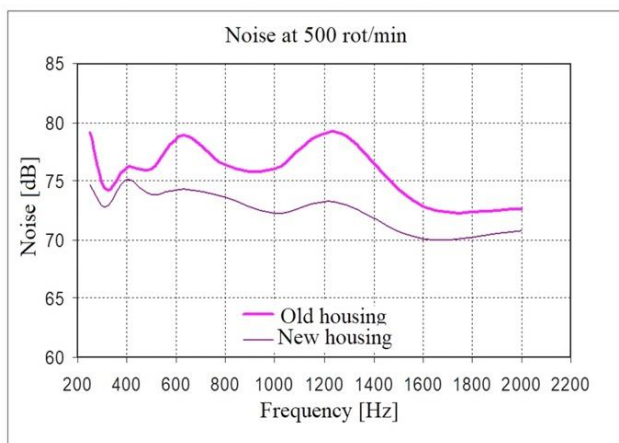


Figure 34. Lp sound pressure level diagrams for left side surface at 500 and 1000 rpm.

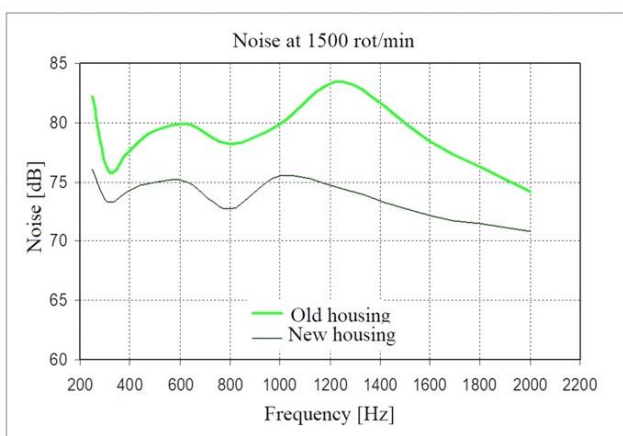


Figure 35. Lp sound pressure level diagrams for left side surface at 1500 and 2000 rpm.

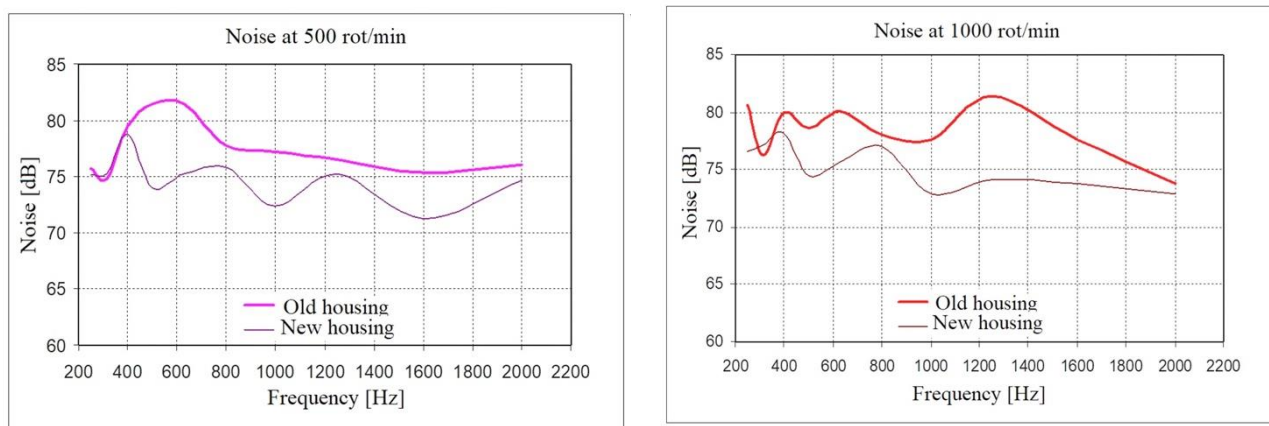


Figure 36. Lp sound pressure level diagrams for right side surface at 500 and 1000 rpm.

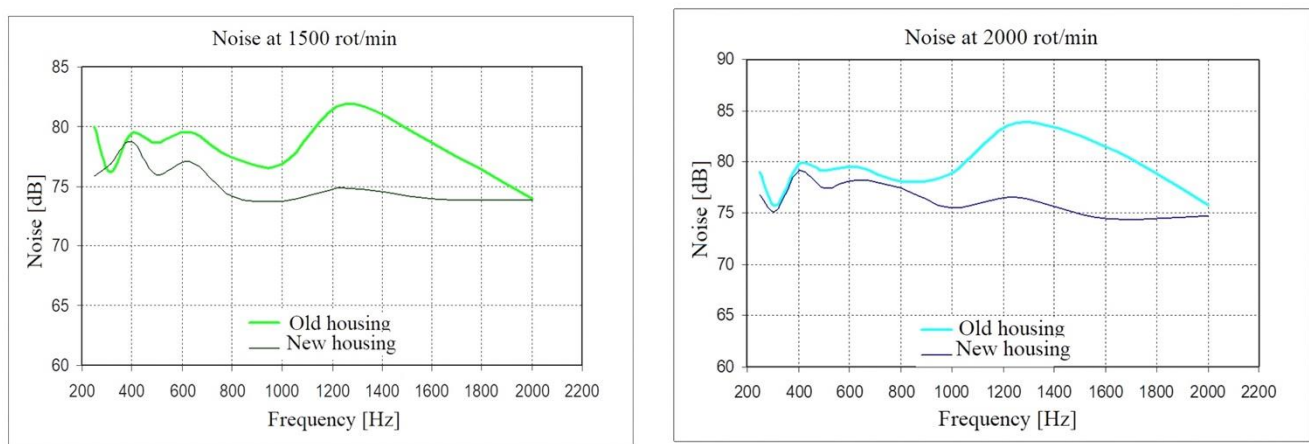


Figure 37. Lp sound pressure level diagrams for right side surface at 1500 and 2000 rpm.

7. Discussions

From the analysis of the results obtained after performing the experiments on the two adder boxes and presented in this paper, the following can be summarized:

1. Measurement and experimental analysis of accelerations on the surfaces of adder boxes
 - The accelerations measured in the three points on the front surface of the new version adder box are approximately 20% lower than the accelerations measured on the front surface of the old version adder box.
 - In the power take-off area, on the front surface of the two summing boxes, the measured accelerations have close values.
 - The accelerations measured in the three points on the rear surface of the new variant adder box are approximately 30% lower than the accelerations measured on the rear surface of the old variant adder box.
 - In the power take-off area, on the rear surface of the two adder boxes, the accelerations measured on the surface of the new version box are 25–30% lower than the accelerations measured on the surface of the old version adder box.
 - In the measuring points in the power take-off area (points 3 and 6), there is a 25% decrease in accelerations on the adder box, the new variant at a speed of 1000 rpm.
 - In Figure 38 are presented, in summary, the accelerations measured on the two summation and distribution boxes at the six measurement points at the four test regimes.
2. Determining the speeds on the surfaces of the summing boxes

- The speeds determined in the three points on the front surface of the new version adder box are approximately 15% lower than the speeds determined for the old version adder box.
 - In the power take-off area (point No. 3), on the front surface of the two adder boxes, the speeds measured on the new version adder box are 20% lower than the speeds measured on the old version adder box.
 - The speeds measured in the three points on the rear surface of the new version adder box are on average 25% lower than the speeds measured on the rear surface of the old version adder box.
 - In the area of the power take-off, on the back surface of the two adder boxes, the speeds measured on the surface of the new version box are 15–20% lower than the speeds measured on the surface of the old version adder box.
 - At the measuring points in the power take-off area (points 3 and 6), a 15% decrease of the speeds on the summing box is observed, the new variant at speeds of 500 and 1000 rpm.
 - In Figure 39 are presented, in summary, the speeds measured on the two summation boxes at the six measurement points at the four test regimes.
 - At the measuring points in the area of the power take-off (points 3 and 6), a 15% decrease of the speeds on the summing box is observed, the new variant at speeds of 500 and 1000 rpm.
3. Determining the displacements on the surfaces of the summing boxes
- The displacements measured in the three points on the front surface of the new variant adder box are approximately 15% smaller than the measured displacements on the front surface of the old variant adder box.
 - In the power take-off area (point No. 3), on the front surface of the two adder boxes, the displacement measured on the adder box of the new version is 15% smaller than the displacement measured on the adder box of the old version.
 - The displacements measured in the three points on the rear surface of the new variant adder box are on average 30% smaller than the displacements measured on the rear surface of the old variant adder box.
 - In the area of the power take-off (point 6), on the back surface of the two adder boxes, the displacements measured on the surface of the new variant box are 30% smaller than the displacements measured on the surface of the old variant adder box.
 - At the measuring points in the power take-off area (points 3 and 6), there is a 10% decrease in displacements on the adder box, the new variant at speeds of 500 and 1000 rpm.
 - In Figure 40 are presented, in summary, the displacements measured on the two summation boxes at the six measurement points at the four test regimes.
4. Measurement and experimental analysis of noise radiated by the surfaces of adder gearboxes
- (a) Noise radiated from the front surface of the summing boxes:
- At a speed of 500 rpm, for the dominant resonant frequencies of 395, 660, and 1600 Hz (determined in Section 5), the noise radiated by the new variant adder box decreased by 8% compared to the noise radiated by the old adder box.
 - At the speed of 1000 rot/min, for the dominant resonant frequencies of 395 and 660 Hz, the noise radiated by the new variant adder box decreased by 10% compared to the noise radiated by the old adder box.
 - At a speed of 1000 rpm, for the frequency of 1600 Hz, we notice a decrease of 6–7% in the noise radiated by the new version summing box.
 - At a speed of 1000 rpm, for the new variant adder box, a constant noise level around 73 dB for the entire frequency range 30–2000 Hz is observed.

- At a speed of 1500 rot/min, for the dominant resonant frequencies of 395 and 660 Hz, the noise radiated by the new variant adder box decreased by 7% compared to the noise radiated by the old adder box.
 - At the speed of 1500 rot/min, for the frequency of 1600 Hz, we observe a decrease of 9% of the noise radiated by the new version summing box.
 - At a speed of 1500 rot/min, for the new variant adder box is observed a noise leveling around 72 dB for the whole frequency range 30–2000 Hz.
 - At a speed of 2000 rpm, for the dominant resonant frequencies of 395, 660, and 1600 Hz, the noise radiated by the new variant box decreased by 6% compared to the noise radiated by the old sum box.
 - At the speed of 2000 rot/min, for the new variant adder box is observed a constant of the noise level around 75 dB for the whole frequency range 30–2000 Hz.
- (b) Noise radiating from the rear surface of the summing boxes:
- At a speed of 500 rpm, for the dominant resonant frequencies of 395, 600, and 1550 Hz (determined in Section 5), the noise radiated by the new variant adder box decreased by 5% compared to the noise radiated by the old adder box.
 - At a speed of 1000 rot/min, for the dominant resonant frequencies of 395 and 600 Hz, the noise radiated by the new version box decreased by 10% compared to the noise radiated by the old box.
 - At a speed of 1000 rpm, for the frequency of 1550 Hz, we observe a decrease of 12% of the noise radiated by the new version summing box.
 - At a speed of 1000 rpm, for the new variant adder box is observed a constancy of the noise level around 75 dB for the whole frequency range 30–2000 Hz.
 - At a speed of 1500 rot/min, for the dominant resonant frequencies of 395, 600, and 1550 Hz, the noise radiated by the new variant adder box decreased by 9% compared to the noise radiated by the old adder box.
 - At the speed of 1500 rot/min, for the frequency of 1600 Hz, we observe a decrease of 9% of the noise radiated by the new version summing box.
 - At a speed of 1500 rot/min, for the new variant adder box is observed a noise leveling around 75 dB for the whole frequency range 30–2000 Hz.
 - At the speed of 2000 rot min, for the dominant resonant frequencies of 395, 600, and 1550 Hz, the noise radiated by the new adder box decreased by 7% compared to the noise radiated by the old adder box.
 - At the speed of 2000 rpm, for the new variant adder box, there is a constant noise level around 75 dB for the whole frequency range 30–2000 Hz with a slight increase to 80 dB around the frequency of 1600 Hz.
- (c) Noise radiated by the lateral surfaces of the summing boxes:
- For the whole range of speeds (500, 1000, 1500, and 2000 rpm) and the whole range of frequencies (30–2000 Hz), the noise radiated by the new variant adder box decreased by 7–10% compared to the noise radiated by the old adder box.
 - For the new variant adder box, a noise level between 70 dB and 75 dB is observed for the whole frequency range 30–2000 Hz.
 - Finally, by implementing the proposals for the constructive modification of the adder box, it can be stated that:
 - By removing the large cover assembled by screws, inserting the rods, and reinforcing plates inside the housing, a new variant of the housing structure was stiffened, a proposed objective for reducing the structural noise of the housing.

- The vibration level of the structure and implicitly of the adder box as a whole was reduced.
- The noise produced by the adder box in the new version decreased, on average, by 10–15% compared to the noise produced by the adder box in the old version.
- A constancy was obtained within limited limits (70–75 dB) of the noise level produced by the new version adder box compared to the old version adder box.
- A simplification of the manufacturing technology was obtained and implicitly a reduction of the labor and of the assembly time of the adder box.
- A reduction of the mass of the adder box was obtained with the new variant by approximately 5%, in this phase being relatively little, but the experiments that will follow regarding the achievement of the future objectives of the thesis may achieve a significant reduction of the mass of the adder and distribution box ensemble.

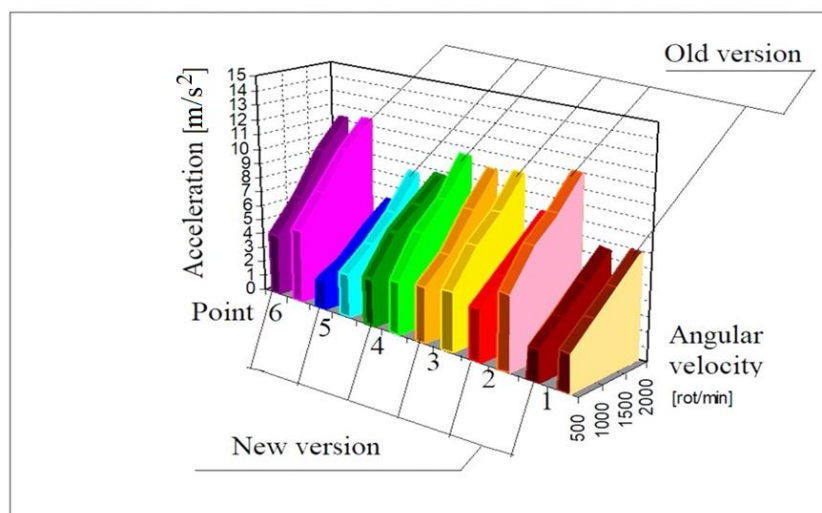


Figure 38. Synthesis of the acceleration values measured on the housings of the two adder gearboxes.

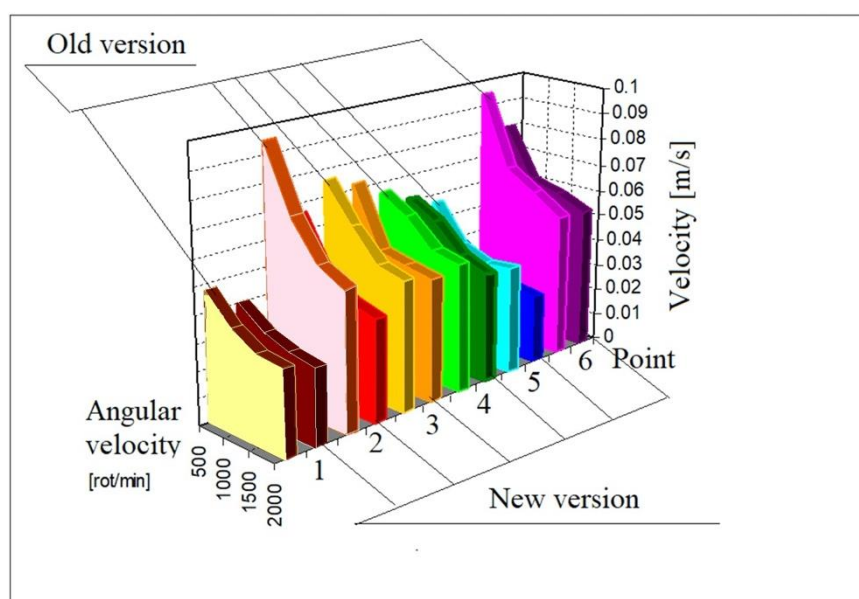


Figure 39. Synthesis of velocities measured on the housings of the two adder gearboxes.

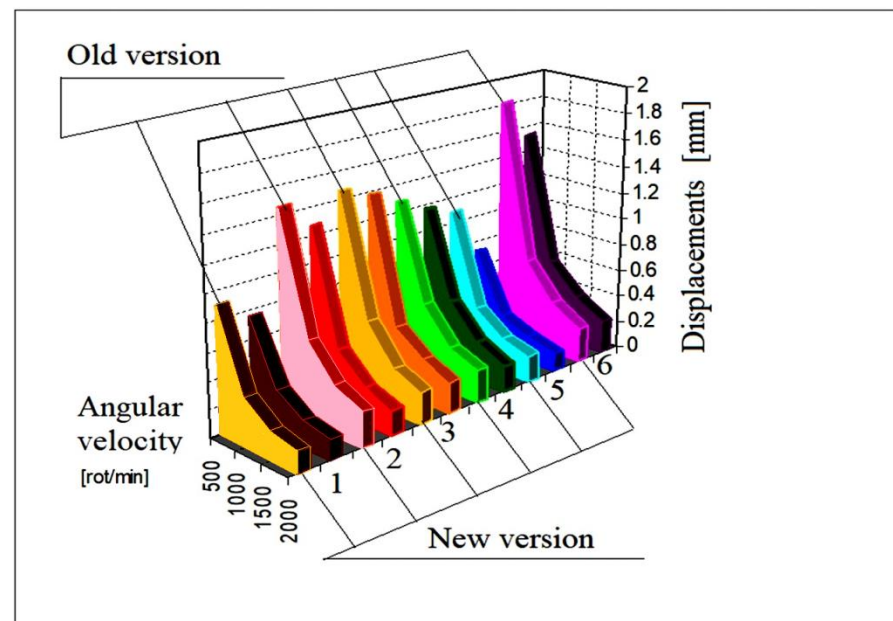


Figure 40. Synthesis of displacements measured on the housings of the two adder gearboxes.

8. Conclusions

The vehicle is a complex mechanical system that, during operation, generates a wide spectrum of vibrations. Much of their energy is radiated outward in the form of sound waves (or noise). The problem of reducing the noise generated by vehicles is an objective of great interest in the world of designers and builders. The reduction of the structural noise of the components creates not only the reduction of the air noise but also the increase in reliability and the diminishment or even elimination of defects such as cracks, deformations, misalignments, etc.

Because modeling and computational determination of radiated noise are difficult, it is necessary that the results obtained be followed by experimental determinations of noise and validation of the models used. The paper presented:

- Analysis of the causes and noise sources of the summing gearboxes.
- Analysis of the noise transmission mechanism in the housing structure of the adder and distribution box.
- Structural and modal analysis of the gearbox housing with the finite element method.
- Experimental determination of the basic parameters of the vibration of the box structure of the summing box (resonant frequencies, amplitudes of vibration displacements of the structure surface, and their distribution on the analyzed surface).
- Analysis of the results of the experimental determinations and presentation of the solutions for modifying the case of the summing box.
- Comparative experimental determinations made by stand testing the adder box with the existing case and the adder box with the modified case.
- Analysis of the results of comparative experiments and validation of the changes made on the housing that led to the reduction of the structure noise and the improvement of the constructive solution.

The analysis of the results of the experimental determinations presented in Section 3 led to the redesign of the adder box housing. Solutions have been proposed to stiffen the structure of the housing, thus resulting in a reduction of its structural noise.

The design and construction of the housing in the improved version required the validation of the constructive solution. Thus, comparative tests were performed on the test stand for both housing variants (existing and improved). The tests performed and the comparison of the results obtained for the summing boxes in the old and new version were presented.

The test results showed that by stiffening the box housing, the vibration level was reduced and, implicitly, the structural noise of the summing box housing was reduced.

For the experiments performed, a test stand was used for:

- Measurement and experimental analysis of the noise radiated by the surfaces of the adder box housing in a state of simulated vibration for the same frequency range.
- Determining the resonant frequencies of the structure of the summing box to which correspond maximum values of the noise radiated by its surfaces.
- Experimental determination of the amplitudes of the vibration displacements of the surface of the summing box, their distribution on the analyzed surface, and the location of the areas that present maximum amplitudes.
- Establishing the program of comparative tests on the stand for both variants of summing boxes (the old version box equipped with the existing case and the new version box equipped with the modified case).
- Experimental determination on the stand of the vibration parameters of the old and new variant summing boxes for the running-in test (accelerations, speeds, and displacements in six points on the carcass surfaces).
- Experimental determination on the stand of the noise radiated by the surfaces of the old and new variant summing boxes at the running-in test (noise radiated by the surface of the front, rear, lateral left, and lateral right).
- Processing the recorded results and comparing them in order to validate the proposed solution for modifying the case of the summing box.

The studied chassis has seven axles of which five are drive axles. With two engines, two gearboxes, a gearbox, and a wide range of units and drilling rigs, this chassis becomes very heavy. For this chassis and therefore implicitly also for the adder and distribution box, the next goal in terms of reliability is the reduction of the mass.

Therefore, for the adder box, we have at least two future research directions, increasing the reliability and reducing the total mass, that have been followed and carried out in this paper. Further research should include:

- Improving the system of fastening and fixing the chassis, improving the damping being an efficient and consistent procedure for reducing structural noise.
- Improving the lubrication system, where we have many components both inside and outside the adder box. A thorough study, supported by in-service behavior information, followed by improvement solutions, tests, and experiments, can reduce the structural noise of the box. It is possible to intervene and improve the fixing of the central ramp inside, the fixing of the inner and outer pipes, the fixing and drive of the pump, and the fixing of the filters on the housing.
- Similar to the lubrication system, a research direction can also be the oil cooling–heating system, taking into account that this adder box works in an environment with high temperature fluctuations.
- Improving gears and smooth operation of bearings, other powerful sources that generate structural noise. Basically, the transmission ratio can be kept for gears, but the module, the gear angle and the specific displacements, the surface quality, the lubrication quality, etc., can be improved.

In order to reduce material consumption, fuel, labor, and practical costs, it is necessary to research the adder box from a constructive point of view. Paradoxically, reducing the level of structural noise of a product can be done by adding mass. As we saw in Section 2, the characteristics of the material used in the box housing have a fairly high level of resistance limit in operation. From the structural analysis by the finite element method, presented in Section 3, we can note that the maximum level of unit stresses in the carcass structure (walls) are much lower than the material strength limit, so there are reservations in the case of carcass redesign. The new housing may be lighter but must maintain high rigidity so as not to be a source of structural noise that affects the functionality and reliability of the box.

Author Contributions: Conceptualization, N.S. and S.V.; methodology, N.G., N.S. and S.V.; software, N.S. and M.M.; validation, N.G., S.V. and M.M.; formal analysis, N.G. and M.M.; investigation, N.S.; resources, S.V.; data curation, N.S. and S.V.; writing—original draft preparation, N.S. and S.V.; writing—review and editing, S.V. and M.M.; visualization, N.G., S.V. and M.M.; supervision, S.V.; project administration, S.V. and M.M.; funding acquisition, S.V. All authors have read and agreed to the published version of the manuscript.

Funding: This research received no external funding.

Institutional Review Board Statement: Not applicable.

Informed Consent Statement: Not applicable.

Data Availability Statement: Not applicable.

Acknowledgments: Not applicable in this paper.

Conflicts of Interest: The authors declare no conflict of interest.

Appendix A

Table A1. The measured accelerations on six points of the adder gearbox.

Measurement Point	Angular Speed [rot/min]	Acceleration [m/s ²]		Decreasing/Increasing [%]
		CSD Old	CSD New	
1	500	2.5	2.1	19.04 ↓
	1000	4	3.5	14.28 ↓
	1500	5.3	5	6 ↓
	2000	7	6.6	6.06 ↓
2	500	5	3.5	42.85 ↓
	1000	7.5	5	50 ↓
	1500	9	6.5	38.46 ↓
	2000	11	8	37.5 ↓
3	500	4	3.8	5.26 ↓
	1000	6.5	5.3	22.64 ↓
	1500	8.1	7.8	3.84 ↓
	2000	10.2	10	2 ↓
4	500	3.5	3.2	9.37 ↓
	1000	6.3	5.8	8.62 ↓
	1500	8	7.2	11.11 ↓
	2000	10.5	8.7	20.68 ↓
5	500	3	2	50 ↓
	1000	4.5	3.1	45.16 ↓
	1500	6.2	4.7	31.91 ↓
	2000	8.5	6.1	39.34 ↓
6	500	5	4.2	19.04 ↓
	1000	7.2	6.4	12.5 ↓
	1500	9.7	9.3	4.3 ↓
	2000	11.5	11.2	2.67 ↓

Table A2. The determined velocities accelerations on six points of the adder gearbox.

Measurement Point	Angular Velocity [rot/min]	Velocity [m/s]		Decreasing/Increasing [%]
		CSD Old	CSD New	
1	500	0.048	0.040	20 ↓
	1000	0.038	0.033	15.15 ↓
	1500	0.033	0.030	10 ↓
	2000	0.032	0.028	14.28 ↓
2	500	0.095	0.066	43.93 ↓
	1000	0.071	0.047	51.06 ↓
	1500	0.057	0.041	39.02 ↓
	2000	0.052	0.038	36.84 ↓

Table A2. Cont.

Measurement Point	Angular Velocity [rot/min]	Velocity [m/s]		Decreasing/Increasing [%]
		CSD Old	CSD New	
3	500	0.076	0.072	5.55 ↓
	1000	0.062	0.050	24 ↓
	1500	0.051	0.048	6.25 ↓
	2000	0.048	0.046	4.34 ↓
4	500	0.066	0.061	8.19 ↓
	1000	0.060	0.055	9.09 ↓
	1500	0.050	0.045	11.11 ↓
	2000	0.048	0.041	17.07 ↓
5	500	0.057	0.038	50 ↓
	1000	0.043	0.029	48.27 ↓
	1500	0.039	0.027	44.44 ↓
	2000	0.040	0.026	53.84 ↓
6	500	0.095	0.080	18.75 ↓
	1000	0.068	0.061	11.47 ↓
	1500	0.061	0.058	5.17 ↓
	2000	0.054	0.053	1.88 ↓

Table A3. The determined displacements on six points of the adder gearbox.

Measurement Point	Angular Velocity [rot/min]	Displacement [mm]		Decreasing/Increasing [%]
		Old Box	New Box	
1	500	0.91	0.76	19.73 ↓
	1000	0.36	0.32	12.5 ↓
	1500	0.21	0.20	5 ↓
	2000	0.15	0.15	0 ↓
2	500	1.46	1.27	14.96 ↓
	1000	0.59	0.45	31.11 ↓
	1500	0.36	0.26	38.46 ↓
	2000	0.25	0.18	38.88 ↓
3	500	1.46	1.38	5.79 ↓
	1000	0.59	0.48	22.91 ↓
	1500	0.32	0.31	3.22 ↓
	2000	0.23	0.22	4.5 ↓
4	500	1.27	1.16	9.48 ↓
	1000	0.57	0.53	7.54 ↓
	1500	0.32	0.29	10.34 ↓
	2000	0.23	0.19	21.05 ↓
5	500	1.09	0.73	49.31 ↓
	1000	0.41	0.28	46.42 ↓
	1500	0.25	0.19	31.57 ↓
	2000	0.19	0.14	35.71 ↓
6	500	1.82	1.53	18.95 ↓
	1000	0.65	0.58	12.06 ↓
	1500	0.39	0.37	5.4 ↓
	2000	0.26	0.25	4 ↓

Table A4. Noise level on the front surface of housing.

Frequency [Hz]	Angular Velocity [rot/min]	CSD Old Noise [dB]	CSD New Noise [dB]	Decreasing/Increasing Noise Level [%]
250	500	75.7	74.7	1.33 ↓
	1000	80.6	75	7.46 ↓
	1500	80	76.1	5.12 ↓
	2000	79	76.5	3.26 ↓

Table A4. Cont.

Frequency [Hz]	Angular Velocity [rot/min]	CSD Old Noise [dB]	CSD New Noise [dB]	Decreasing/Increasing Noise Level [%]
315	500	74.8	72.8	2.74 ↓
	1000	76.2	73	4.38 ↓
	1500	76.2	73.3	3.95 ↓
	2000	75.8	73.6	2.98 ↓
400	500	79.5	76.4	4.05 ↓
	1000	79.9	73.6	8.55 ↓
	1500	79.4	74.3	6.86 ↓
	2000	79.8	74.3	7.40 ↓
500	500	81.5	73.9	10.28 ↓
	1000	78.6	74	6.21 ↓
	1500	78.6	74.9	4.93 ↓
	2000	79.2	75.6	4.76 ↓
630	500	81.4	74.3	9.55 ↓
	1000	80.1	74.2	7.95 ↓
	1500	79.5	74.9	6.14 ↓
	2000	79.5	75.6	5.15 ↓
800	500	77.8	73.7	5.56 ↓
	1000	78	73.6	5.97 ↓
	1500	77.4	72.7	6.46 ↓
	2000	78.1	74.3	5.11 ↓
1000	500	77.2	72.3	6.77 ↓
	1000	77.6	72.6	6.88 ↓
	1500	76.9	75.5	1.85 ↓
	2000	78.9	74.8	5.48 ↓
1250	500	76.5	73.2	4.50 ↓
	1000	81.4	72.7	11.96 ↓
	1500	81.9	74.4	10.08 ↓
	2000	83.8	75.8	10.55 ↓
1600	500	75.4	70.1	7.56 ↓
	1000	77.6	71.9	7.92 ↓
	1500	78.6	72.2	8.86 ↓
	2000	81.5	78.5	3.82 ↓
2000	500	76.1	70.8	7.48 ↓
	1000	73.8	72.9	1.23 ↓
	1500	73.9	70.8	4.37 ↓
	2000	75.8	72.2	4.98 ↓

Table A5. Noise level on the rear surface of housing.

Frequency [Hz]	Angular Velocity [rot/min]	CSD Old Noise [dB]	CSD New Noise [dB]	Decreasing/Increasing Noise Level [%]
250	500	79.2	73.5	7.75 ↓
	1000	77	73.9	4.19 ↓
	1500	76.3	74.6	2.28 ↓
	2000	76	75.4	0.79 ↓
315	500	74.3	72.5	2.48 ↓
	1000	77.3	73	5.89 ↓
	1500	77.8	74.3	4.71 ↓
	2000	76.9	74.5	3.22 ↓
400	500	76.2	74.3	2.55 ↓
	1000	80.9	78.1	3.58 ↓
	1500	81.3	78.9	3.04 ↓
	2000	81.2	78.8	3.04 ↓
500	500	76.5	76	0.65 ↓
	1000	84.6	77.3	9.44 ↓
	1500	85.7	79	8.48 ↓
	2000	85.3	79.2	7.70 ↓

Table A5. Cont.

Frequency [Hz]	Angular Velocity [rot/min]	CSD Old Noise [dB]	CSD New Noise [dB]	Decreasing/Increasing Noise Level [%]
630	500	78.9	74.6	5.76 ↓
	1000	83.1	74.2	11.99 ↓
	1500	83.6	75.5	10.72 ↓
	2000	83.5	76.8	8.72 ↓
800	500	76.4	73.4	4.08 ↓
	1000	81	75.5	7.28 ↓
	1500	80.8	73.2	10.38 ↓
	2000	81.7	74.6	9.51 ↓
1000	500	76	72	5.55 ↓
	1000	80.8	72.8	10.98 ↓
	1500	81.3	74.6	8.98 ↓
	2000	82	74.2	10.51 ↓
1250	500	79.1	72.2	9.55 ↓
	1000	80.6	72.8	10.71 ↓
	1500	82.2	75.8	8.44 ↓
	2000	83.1	77.1	7.78 ↓
1600	500	72.8	70.5	3.26 ↓
	1000	82	73.1	12.17 ↓
	1500	82	73.3	11.86 ↓
	2000	85.1	79.6	6.90 ↓
2000	500	72.6	71.3	1.82 ↓
	1000	77.5	71.6	8.24 ↓
	1500	77.9	74	5.27 ↓
	2000	80	76.9	4.03 ↓

Table A6. Noise level on the lateral left surface of housing.

Frequency [Hz]	Angular Velocity [rot/min]	CSD Old Noise [dB]	CSD New Noise [dB]	Decreasing/Increasing Noise Level [%]
250	500	79.2	74.7	6.02 ↓
	1000	77	75	2.66 ↓
	1500	82.2	76.1	8.01 ↓
	2000	81.1	76.5	6.01 ↓
315	500	74.3	72.8	2.06 ↓
	1000	77.3	73	5.89 ↓
	1500	76	73.3	3.68 ↓
	2000	75.7	73.6	2.85 ↓
400	500	76.2	75.1	1.46 ↓
	1000	80.9	73.6	9.91 ↓
	1500	77.6	74.3	4.44 ↓
	2000	78.2	74.3	5.24 ↓
500	500	76.1	73.9	2.97 ↓
	1000	84.6	74	14.32 ↓
	1500	79.3	74.9	5.87 ↓
	2000	79.2	75.6	4.76 ↓
630	500	78.9	74.3	6.19 ↓
	1000	83.1	74.2	11.99 ↓
	1500	79.9	74.9	6.67 ↓
	2000	80.4	75.6	6.34 ↓
800	500	76.4	73.7	3.66 ↓
	1000	81	73.6	10.05 ↓
	1500	78.2	72.7	7.56 ↓
	2000	79.2	74.3	6.59 ↓
1000	500	76	72.3	5.11 ↓
	1000	80.8	72.6	11.29 ↓
	1500	79.9	75.5	5.82 ↓
	2000	82.2	74.8	9.89 ↓

Table A6. Cont.

Frequency [Hz]	Angular Velocity [rot/min.]	CSD Old Noise [dB]	CSD New Noise [dB]	Decreasing/Increasing Noise Level [%]
1250	500	79.1	73.2	8.06 ↓
	1000	80.6	72.7	10.86 ↓
	1500	83.4	74.4	12.09 ↓
	2000	85.5	75.8	12.79 ↓
1600	500	72.8	70.1	3.85 ↓
	1000	82	71.9	14.04 ↓
	1500	78.4	72.2	8.58 ↓
	2000	81	78.5	3.18 ↓
2000	500	72.6	70.8	2.54 ↓
	1000	77.5	72.9	6.31 ↓
	1500	74.2	70.8	4.80 ↓
	2000	76.3	72.2	5.67 ↓

Table A7. Noise level on the lateral right surface of housing.

Frequency [Hz]	Angular Velocity [rot/min.]	CSD Old Noise [dB]	CSD New Noise [dB]	Decreasing/Increasing Noise Level [%]
250	500	75.7	75.1	0.79 ↓
	1000	80.6	76.6	5.22 ↓
	1500	80	75.9	5.40 ↓
	2000	79	76.8	2.86 ↓
315	500	74.8	75.3	0.66 ↓
	1000	76.2	77.1	1.18 ↓
	1500	76.2	76.8	0.78 ↓
	2000	75.8	75.2	0.79 ↓
400	500	79.5	78.8	0.88 ↓
	1000	79.9	78.2	2.17 ↓
	1500	79.4	78.8	0.76 ↓
	2000	79.8	79.2	0.75 ↓
500	500	81.5	74	10.13 ↓
	1000	78.6	74.5	5.50 ↓
	1500	78.6	76	3.42 ↓
	2000	79.2	77.5	2.19 ↓
630	500	81.4	75.2	8.24 ↓
	1000	80.1	75.7	5.81 ↓
	1500	79.5	77.1	3.11 ↓
	2000	79.5	78.2	1.66 ↓
800	500	77.8	75.8	2.63 ↓
	1000	78	77	1.29 ↓
	1500	77.4	74.2	4.31 ↓
	2000	78.1	77.5	0.77 ↓
1000	500	77.2	72.4	6.62 ↓
	1000	77.6	72.9	6.44 ↓
	1500	76.9	73.7	4.34 ↓
	2000	78.9	75.5	4.50 ↓
1250	500	76.5	75.3	1.59 ↓
	1000	81.4	74.1	9.85 ↓
	1500	81.9	74.8	9.49 ↓
	2000	83.8	76.5	9.54 ↓
1600	500	75.4	71.2	5.89 ↓
	1000	77.6	73.8	5.14 ↓
	1500	78.6	73.9	6.35 ↓
	2000	81.5	74.5	9.39 ↓
2000	500	76.1	74.7	1.87 ↓
	1000	73.8	72.9	1.23 ↓
	1500	73.9	73.8	0.13 ↓
	2000	75.8	74.8	1.33 ↓

References

1. Soami, P. Modeling Vibration and Noise in a Gearbox. *Mech. Eng.* **2018**, *140*, 22–24.
2. Furch, J.; Tran, C.V. Dynamics simulation of mechanical gearbox vibration. In Proceedings of the 10th International Scientific Conference on Aeronautics, Automotive and Railway Engineering and Technologies (BulTrans), Sozopol, Bulgaria, 15–17 September 2018; Volume 234. AR 02002. [[CrossRef](#)]
3. Elisabeth, K.; John, L.; Lars, H.; Magnus, K.; Jing, L. Vibration-based Condition Monitoring of Heavy Duty Machine Driveline Parts: Torque Converter, Gearbox, Axles and Bearings. *Int. J. Progn. Health Manag.* **2019**, *10*. [[CrossRef](#)]
4. Wu, H.; Wu, P.B.; Xu, K.; Li, J.C.; Li, F.S. Research on Vibration Characteristics and Stress Analysis of Gearbox Housing in High-Speed Trains. *IEEE Access* **2019**, *7*, 102508–102518. [[CrossRef](#)]
5. Batizi, V.; Likhachev, D. Mass-geometric parameters improvement of gearbox by using vibration analysis. In Proceedings of the 14th International Conference on Vibration Engineering and Technology of Machinery (VETOMAC XIV), Lisbon, Portugal, 10–13 September 2018; Volume 211. AR 06002. [[CrossRef](#)]
6. Guo, W.; Chen, C.; Xiao, N.C. Dynamic vibration feature analyses for a two-stage planetary gearbox with a varying crack using a rigid-flexible coupled model. *J. Intell. Fuzzy Syst.* **2018**, *34*, 3869–3880. [[CrossRef](#)]
7. Furch, J.; Glos, J.; Nguyen, T.T. Modelling and Simulation of Mechanical Gearbox Vibrations. In Proceedings of the International Conference 20th International Scientific Conference on Transport Means, Juodkrante, Lithuania, 5–7 October 2016; pp. 133–139.
8. Kucukay, F.; Pfeiffer, F. Clattering Vibrations in Gearboxes of Motor-Vehicles. *Ingenieur Arch.* **1986**, *56*, 25–37. [[CrossRef](#)]
9. Astridge, D.G. Gearbox Noise and Vibration- Review of Opportunities for Improving Safety and Reliability. In Proceedings of the Institution of Mechanical Engineers Series. 1st International Conf on Gearbox Noise and Vibration, Univ. Cambridge, Cambridge, UK, 9–11 April 1990; pp. 11–18.
10. Vlase, S. A Method of Eliminating Lagrangian-Multipliers from the Equation of Motion of Interconnected Mechanical Systems. *J. Appl. Mech. Trans. ASME* **1987**, *54*, 235–237. [[CrossRef](#)]
11. Vlase, S.; Teodorescu, P.P. Elasto-Dynamics of a Solid with a General "Rigid" Motion using FEM Model Part I. Theoretical Approach. *Rom. J. Phys.* **2013**, *58*, 872–881.
12. Scutaru, M.L.; Vlase, S.; Marin, M.; Modrea, A. New analytical method based on dynamic response of planar mechanical elastic systems. *Bound. Value Probl.* **2020**, *2020*, 104. [[CrossRef](#)]
13. Wang, Q.; Shen, R.Y. Study on Vibration & Noise of Gearbox. In Proceedings of the 14th International Congress on Acoustics (ICA 14), Beijing, China, 3–10 September 1992; Volumes 1–4. pp. 679–680.
14. Tuma, J. Analysis of Gearbox Vibration in Time Domain. In Proceedings of the Institute of Acoustics, Euro Noise 92, London, UK, 14–18 September 1992; Volume 14, pp. 597–604.
15. Choy, F.K.; Ruan, Y.F.; Tu, Y.K.; Zakrajsek, J.J.; Townsend, D.P. Modal-Analysis of Multistage Gear Systems Coupled with Gearbox Vibration. *J. Mech. Des.* **1992**, *114*, 486–497. [[CrossRef](#)]
16. Sargeant, M.; Stone, B.J. Coupled torsional and transverse vibration of gearboxes. In Proceedings of the 3rd International Symposium on Multi-Body Dynamics -Monitoring and Simulation Techniques, Loughborough, UK, 12–13 July 2004; pp. 299–309.
17. Guan, Y.H.; Shepard, W.S.; Lim, T.C.; Li, M. Experimental analysis of an active vibration control system for gearboxes. *Smart Mater. Struct.* **2004**, *13*, 1230–1237. [[CrossRef](#)]
18. Guan, Y.H.; Lim, T.C.; Shepard, W.S. Experimental study on active vibration control of a gearbox system. *J. Sound Vib.* **2005**, *282*, 713–733. [[CrossRef](#)]
19. Li, M.F.; Lim, T.C.; Shepard, W.S.; Guan, Y.H. Experimental active vibration control of gear mesh harmonics in a power recirculation gearbox system using a piezoelectric stack actuator. *Smart Mater. Struct.* **2005**, *14*, 917–927. [[CrossRef](#)]
20. Ploger, D.; Zech, P.; Rinderknecht, S. Experimental identification of high-frequency gear mesh vibrations in a planetary gearbox. In Proceedings of the International Conference on Noise and Vibration Engineering (ISMA)/International Conference on Uncertainty in Structural Dynamics (USD), Leuven, Belgium, 19–21 September 2016; pp. 911–924.